RESEARCH STUDY OF LIGHT EMISSION CAUSED BY PRESSURE FLUCTUATIONS IN ROCKET ENGINES

B. Hornstein
C. Budnik
W. Courtney

Physics Department

RMD Report No. 5520-F

March 1966

Final Report
1 January 1965 - 31 December 1965

Contract AF 49(638)-1505

Thiokol
CHEMICAL CORPORATION
REACTION MOTORS DIVISION
DENVILLE, NEW JERSEY

Thiokol
REACTION MOTORS DIVISION

RESEARCH STUDY OF LIGHT EMISSION CAUSED BY PRESSURE FLUCTUATIONS IN ROCKET ENGINES

B. Hornstein
C. Budnik
W. Courtney

Physics Department

RMD Report No. 5520-F

March 1966

Final Report
1 January 1965 - 31 December 1965

Contract AF 49(638)-1505

Approved by

W. G. Courtney
Acting Manager, Physics Department

D. J. Mann
Director of Research

THIOKOL CHEMICAL CORPORATION
REACTION MOTORS DIVISION
DENVILLE, NEW JERSEY 07834

ABSTRACT

This program was to investigate the usefulness of spectroscopy as a diagnostic technique for studying combustion instability in a rocket chamber. Main emphasis was given to investigating pressure and the 3064Å (OH) and 4315Å (CH) emission as a function of time in order to study the time lag between pressure and emission. The 1100 cps longitudinal mode and the 7100 cps tangential mode in a cylindrical motor 3 inches in diameter and 16 inches long were investigated. Two propellant systems were used, a premixed methane-air gaseous system and a liquid pentane-gaseous air system.

Optical results were limited in reproducibility, perhaps because of local turbulent combustion phenomena. Time-averaged spectra indicated no other strong spectral lines in the 2800-4400Å range but did indicate that a CO + O continuum existed and became more intense as the chamber pressure increased and particularly when non-impinging jet injectors were used with the pentane-air system. This intense CO + O continuum obscures the CH emission and severely limits the usefulness of spectroscopy as a diagnostic tool. The initiation and dampening of the 1100 cps longitudinal mode was briefly studied.

TABLE OF CONTENTS

		Page
	Abstract	ii
I.	Introduction	1
II.	Equipment and Technique	6
	A. General Remarks	6
	B. Combustion Chambers	7
	C. Methane-Air Injectors	8
	D. Pentane-Air Injectors	10
	E. Propellant Flow System	11
	F. Pressure Instrumentation	12
	G. Emission Instrumentation	13
III.	Results	17
	A. General Remarks	17
	B. Premixed Gaseous Methane-Air	17
	1. Pressure Oscillations	18
	2. Initiation and Dampening	19
	3. Deceleration	20
	4. OH and CH Emission	20
	5. Time-Averaged Spectra	21
	C. Liquid Pentane-Air	21
	1. Pressure Oscillations	21
	2. Initiation and Dampening	22
	3. Deceleration	22
	4. OH, CH, and "Total" Emission	23
	5. Time-Averaged Spectra	23
IV.	Discussion	24
V.	Acknowledgments	26
VI.	References	27

FIGURES

Fig. 1. Assembly Drawing of Basic Engine.

Fig. 2. Plexiglas Chamber.

Fig. 3. Uncooled Metal Chamber.

Fig. 4. Kistler Pressure Adapter and Window Modification.

Fig. 5. Quartz Window and Pressure Tap Plate.

Fig. 6. Water-Cooled 12-Port Injector and Uncooled 6-Port Injector for Methane-Air.

Fig. 7. Mirror Port in Injector to View Transverse Mode.

Fig. 8. Methane-Air Injector with Mirror Port.

Fig. 9. Liquid Pentane-Air Injector.

Fig. 10. Spectral Response of RCA Type 1P28 Photomultiplier Tube.

Fig. 11. Transmission of Baird Atomic Interference Filter for OH (0, 0) Band at 3064Å.

Fig. 12. Transmission of Baird Atomic Interference Filter for the CH (0, 0) Band at 4315Å.

Fig. 13. Typical Motion Pictures of Luminosity in Methane-Air and Liquid Pentane-Air Systems.

Fig. 14. Transition from Longitudinal to Tangential Instability with Methane-Air.

Fig. 15. Typical Instability Map for Methane-Air.

Fig. 16. Evidence for Plane Longitudinal Wave with Methane-Air.

Fig. 17. Amplitude of Instability Mode vs. Chamber Pressure for Various Injector Configurations with Methane-Air.

FIGURES (Continued)

Fig. 18. Transverse Mode with Methane-Air Showing 180° Out of Phase Measurement.

Fig. 19. Initiation and Dampening of Longitudinal Mode with Methane-Air.

Fig. 20. Deceleration of Pressure Wave with Methane-Air.

Fig. 21. OH and CH Emission with Methane-Air. Reproducibility and Effect of P_c.

Fig. 22. Time-Average Emission Spectra of Methane-Air.

Fig. 23. Typical Oscilloscope Trace of Longitudinal Mode with Pentane-Air.

Fig. 24. Typical CEC Trace of Longitudinal Mode with Pentane-Air.

Fig. 25. Transverse Mode with Fuel-Rich Pentane-Air.

Fig. 26. OH and CH Emission Lag with Impinging Pentane-Air.

Fig. 27. OH and CH Emission Lag with Impinging Pentane-Air.

Fig. 28. OH and CH Emission Lag with Non-Impinging Pentane-Air.

Fig. 29. Time-Averaged Spectra with Pentane-Air. Effect of Impingement and Chamber Pressure.

Fig. 30. Time-Averaged Spectra with Pentane-Air. Effect of Impingement and Chamber Pressure.

Fig. 31. Time-Averaged Spectra with Pentane-Air. Effect of Impingement and Chamber Pressure.

Fig. 32. Typical Raw Time-Averaged Spectra with Methane-Air and Pentane-Air.

I. INTRODUCTION

It is generally agreed that high-frequency combustion instability in a rocket motor is a coupled process involving energy release feeding a pressure disturbance. The presence of instability thus depends upon how the combustion time is related to (a) natural frequencies in the chamber cavity and (b) the pressure dependence of the combustion rate. However, these parameters of time lag, space lag and interaction coefficient are quantities whose values are not yet describable in terms of reaction kinetics, injection conditions, evaporation times, and recirculation. Thus, empirical engineering "fixes" are usually used in an attempt to cure instability. Such an approach often is successful but is tedious and expensive, and one may hope that a more scientific approach might be more efficient.

Previous work in instability (Ref. 1) has largely been devoted to measuring the pressure oscillations as a function of "engineering" parameters such as chamber geometry and injection configuration. A limited amount of effort has been devoted to investigating the "total" emission during instability, e.g., by conventional photography and wide band phototubes. Results have indicated, for example, that the emission fluctuation lagged the pressure fluctuation by about 1/4 wave length (0.3 millisec), and this lag was interpreted in terms of the general mechanisms whereby the local combustion rate sustains the pressure wave (for example, Ref. 1a). Unfortunately only total radiation emission was

monitored, so that it was not possible to specify the origin of the radiation.

However, spectroscopic techniques have often been used as a "probing" technique to gain insight into the combustion mechanisms and reaction kinetics of laboratory flames (Ref. 2). The question therefore arises whether spectroscopic techniques can supply insight into the combustion lag problem in instability and thereby permit one to relate the effect of pressure fluctuations with kinetic details.

The present program was a fundamental experimental investigation of combustion instability in a laboratory-type rocket motor using spectroscopic techniques to study the spectral variation of light emission that accompanies the pressure fluctuations in the rocket chamber. OH, CH, and "total" emission were initially selected (Ref. 4) as analytical "indicators" of the rate of the combustion reactions resulting from the passage of the pressure wave. Time-averaged spectra were included in later work.

The intensity of the OH radiation (3064Å) from a laboratory flame is reported to be approximately independent of pressure (Ref. 2). CH (4315Å) was included here because it is a non-equilibrium fragment and radiates only from the reaction zone, although the CH intensity from a laboratory flame is reported to decrease with increasing pressure (Ref. 2). The total emission consists of the above emission and also emission due to reactions such as the CO + O continuum and was included here to provide data for comparison emission with Ref. 1a. The time-averaged spectra were included in the hope

that other emission lines might be present and could be used to trace the combustion mechanism.

Results were to be interpreted in terms of spectral emission in relation to chemical heat release and pressure fluctuations in order to gain insight into the kinetic time lag. Hopefully, this understanding would then provide guidelines for modifying the kinetic lag by using inhibitors or modifying the spray parameters and thus minimizing instability in an engine.

This report is the annual report covering the second year of this work under AFOSR Contract AF49(638)-'505. Dr. B. T. Wolfson was the Scientific Officer.

Work during the previous year (Ref. 4) investigated fluctuations in pressure and spectral emission in a small gas-type rocket engine* (50 lbs thrust, 50 to 150 psig). Premixed methane and air were used to avoid the lags associated with physical phenomena such as droplet evaporation kinetics. Longitudinal oscillations of ~1100 cps and transverse oscillations of ~7100 and ~14,000 cps (1st tangential and 1st radial) were observed. The OH and CH emission lagged the longitudinal pressure fluctuation by about 1/5 wave length (0.2 millisec) at low chamber pressure (50-100 psig), but generally no lag was observed at 150 psig chamber pressure. The "total" luminosity normally showed no lag. However, reproducibility was

*The engine was essentially identical to that used by the Purdue investigators (Ref. 3).

very poor. For example, a 0.3 millisec lag in total luminosity was also observed in the present work but only very infrequently. The reason for this poor reproducibility was not clear, although we suspected that instrumentation errors may have accounted for part of the reproducibility problem. Also, data analysis was difficult due to hashy wave forms. The noise component (or the second, third etc. order harmonic) frequently prevents a clear cut indication of the peak of the wave. Therefore true time lag readout was difficult.

The above results with total luminosity generally were somewhat contrary to the consistently-observed 0.3 millisec lag for total luminosity reported by Zucrow et al (Ref. 1a), and the disparity generally seemed to be outside of experimental errors.

In the present year, the work consisted of:

1) a re-examination of OH and CH vs. P fluctuations in the premixed gaseous methane-air system using improved instrumentation. This work was to determine if the previous limited reproducibility was an instrumentational feature or was due to a more fundamental nature,
2) a detailed spectroscopic study of the time-averaged emission from the above methane-air gaseous system, and

3) an exploratory study of pressure and spectral fluctuations in a liquid pentane-gaseous air system in the same rocket engine.

While physical processes in a liquid system (e. g. , evaporation) are notoriously slow, it was hoped that the spectroscopic results obtained with the gaseous methane-air system would supply insight into the liquid pentane system.

The present work has not progressed as rapidly as was hoped. The results of the present year again were plagued with limited reproducibility. This poor reproducibility made it difficult to detect trends in the results and thereby prevented using the present experimental results to test the theories of combustion instability.

This report summarizes the experimental results obtained during the past year.

II. EQUIPMENT AND TECHNIQUE

A. General Remarks

Most work was done with a 50-lb-thrust cylindrical engine measuring 3-inch ID and 16.125 inches long. This configuration essentially matches the configuration used by Zucrow et al (Ref. 1a). A gaseous H_2/O_2 igniter was used. A motor run consisted of a one-second igniter pulse (starting with the propellant feed) followed by 2 to 3 seconds of operation. The engine and injectors were uncooled during the present work.

Two propellant systems were examined, a premixed gaseous methane-air system and a liquid pentane-air system.

Fig. 1 is an assembly drawing of the engine as originally built. Part No. 15 is a sonic plate to decouple the premix chamber from any chamber pressure fluctuations and to prevent possible flame propagation from the chamber to the premix chamber.

Pressure was measured with Kistler transducers and an oscilloscope. A CEC chart recorder was occasionally used in order to monitor a full run. Chart speed was 64 inches/sec, giving 7 cycles/cm on the chart for the 1100 cps oscillation. The usual measuring station usually was 2.8 inches from the injector face. Measuring stations at 4.75, 9 and 13.25 inches were also used to measure deceleration of the longitudinal pressure wave.

Emission in the longitudinal direction was measured with a phototube at the 2.8-inch station (or through a window). Emission in the transverse

direction was measured by placing a mirror in one of the injector holes so that the field of view was down the motor.

Ranges of conditions examined were:

	methane-air	pentane(l)-air
system	premixed gas	liquid-gas
chamber pressure(P_c)	50-150 psig	50-150 psig
O/F	7-14	0.83-1.4 = λ*
gas velocity	126-1030 ft/sec	
propellant temperature	ambient	ambient

The major improvement in instrumentation over the previous year was to use a wave generator to synchronize the scope sweeps for pressure and phototube. Other improvements included using electronic filtering to reduce noise in the pressure trace and using a quartz back window in the spectroscopy instead of a metal plate to reduce the background continuum.

B. Combustion Chambers

Three different uncooled combustion chambers were used in the present work:

1) Plexiglas, 3-inch ID x 1/4-inch wall x 16-1/8 inch long;

2) stainless, same configuration, small window in pressure tap;

3) stainless, same configuration, large diametrically-opposite viewing ports.

* λ = O_2 present in system/O_2 necessary for stoichiometric combustion.

Figs. 2 and 3 show the Plexiglas and small-window motors. The bosses on the #2 chamber were adapted to Kistler No. 628 adapters which were used to mount the Kistler pressure transducers or a sapphire window. The Kistler-mounted window was particularly useful, for any combination of pressure and light measurements could be made by mounting the fittings in any of the identical tapped holes (see Fig. 3). Fig. 4 is an exploded view of the No. 628 adapter, unmodified with transducer and modified to take the 1/4 inch diameter x 2 mm thick Linde sapphire window. As can be seen, the only modifications needed were of the flame cap and the spacer tube.

Chamber #3 used large diametrically-opposite quartz windows with 1/2 inch by 5-1/2 inch of view area. A plate with five holes tapped to receive Kistler pressure transducers could replace the window. Fig. 5 shows the construction of the window and also the pressure plate as used on an older two-section motor. Chamber #3 used the same construction technique on a one-section stainless motor which was otherwise similar to the motor given in Fig. 3.

C. Methane-Air Injectors

Three injectors were used. The original injector was water-cooled and passed the premixed propellants through twelve axial ports equally spaced on a 2.3-inch-diameter circle. The second injector was an uncooled, solid stainless steel plate 0.6 inch thick with six axial ports evenly spaced on a 1.5 inch diameter circle.

The diameter of ports in both injectors could be varied with inserts from 0.070 to 0.200 inches . order to control propellant injection velocity. Fig. 6 shows the downstream face of both injectors, with an insert partially screwed home. The premixed methane-air gas from the cooled injector entered the chamber on a radius near the chamber wall. With the uncooled injector, the gas entered on a radius halfway between the wall and the chamber axis.

The third injector was an uncooled 11-hole injector similar to the original 12-hole injector but one of the holes was converted to a window in order to view down the motor and observe emission during transverse instability. The technique essentially involved placing a 45° mirror at one of the injector holes. Fig. 7 gives a schematic diagram of the geometry. Fig. 8 gives a photograph of the injector face with the mirror and the pressure cap out.

The calculated nominal injection velocity of a stoichiometric methane-air mixture for various injector arrangements are listed below. These velocities are for a 70°F gas stream. Actual velocities were necessarily somewhat higher owing to heat transfer from the chamber gases to the injector face and thus the gas streams, but the actual temperature rise is not known.

METHANE-AIR INJECTION VELOCITIES

Injector Port Diameter, inches	Velocity ft/sec*		
No. ports =	12	11	6
0.200	115	126	230
0.125	297	333	594
0.100	461	503	922
0.070	943	1030	

* 70°F assumed.

Although the injection velocity varies with stoichiometry (i.e. the total gas flow for a given chamber pressure), it is invariant with chamber pressure at a given mixture ratio. This follows from the direct linear pressure dependence of both propellant mass flow and gas density with chamber pressure.

D. Pentane-Air Injector

The pentane-air injector combination used a central spud to spray the liquid pentane radially outward into the air being ejected down the motor from the "standard" 6- or 12-hole air injector. Three types of liquid pentane injectors were used:

+ 1) 6 jets at 45° to the chamber axis

++ 2) 6 jets at 90° to the axis

+, ++ Built in shop

*3) hollow cone at 45 to 90° to the axis.

Fig. 9 shows the injector arrangement and includes the mirror observation port. The diameter of the air port could be any of the values cited above.

The 6-6 fuel-air injector combination could be either impinging or non-impinging, i. e., the pentane streams could either impinge onto or bisect the air streams.

E. Propellant Flow System

The air supply was a permanent 10-bottle cascade containing about 70,000 SCF at 1500 psi.

Methane and hydrogen (igniter fuel) were drawn from standard 1A commercial cylinders.

The flow system was a straightforward arrangement which contained remote controlled dome loaded regulators, solenoid controlled air-operated on-off propellant valves, check valves, and nitrogen purge lines. Flow was metered with calibrated sonic orifices. Sonic operation allowed simple flow control by setting and monitoring only orifice upstream pressure. Orifice downstream pressure was also monitored, but only to insure that the orifice pressure ratio was above the critical for sonic flow.

Pentane in Hoke cylinders was pressurized by nitrogen and regulated by a valve (air operated for quick action). Flowrate was measured through a

*Commercially available Tan-Jet Hollow cone - orifice dia. 0.028 in.

sharp edge orifice at a regulated pressure.

Methane and air orifice upstream and downstream pressures were measured by calibrated Teledyne strain gage transducers and recorded on Brown recorders at 0. 1 in. sec^{-1} chart speed.

Methane and air orifice upstream temperatures were sensed by copper-constantan thermocouples and recorded on Brown recorders at 0. 1 in. sec^{-1}. The propane temperature was the ambient temperature.

F. Pressure Instrumentation

Chamber pressure level was measured by a calibrated Teledyne transducer and recorder on a Brown at 0. 1 in. sec^{-1}. (The Kistler high frequency transducer is not useful for this essentially steady state pressure sensing because of temperature drift and charge leak-off)

The chamber pressure oscillations were measured by a Kistler No. 601 quartz crystal transducer mounted in a No. 628 water cooled adapter. The adapter was mounted in a chamber port cover plate so that the transducer was flush with the inside of the plate. The No. 601 transducer has a pressure range of 0. 5-5000 psi, a natural frequency of 150, 000 cps, and a sensitivity of approximately 0. 5 pCb (picoCoulomb) per psi. The charge output of the transducer was processed by a Kistler No. 566 charge amplifier which has output ranges from 0. 05 mv pCb^{-1} to 100 mv pCb^{-1}. In the water-cooled adapter, the flat response of the Kistler gauge extended only

to about 10,000 cps.

Charge amplifier output was recorded on a Tektronix No. 551 or No. 555 oscilloscope and also on high speed tape in a central instrumentation facility. The transducers were not shock mounted.

G. Emission Instrumentation

"Total" light emission was measured by an RCA Type 1P28 photomultiplier tube. Peak sensitivity is at 3500Å, with 90% of peak at 3000Å (Fig. 10). Useful response extends to about 5500Å (20% of peak). This range is adequate for observing the OH bands (especially the strong (0, 0) head at 3064Å), the CH bands at 3889Å and 4312Å, and the C_2 bands at 4737Å and 5165Å.

The OH (0, 0) emission at 3064Å was measured by the 1P28 tube in conjunction with a Baird Atomic A-11 first order interference filter (Fig. 11). The calibration curve for this filter shows a 16-1/2% transmission at the peak wavelength of 3066Å, with a bandwidth at half-peak of 280Å.

The CH emission at 4312Å was measured with the 1P28 tube and a Baird CH filter which peaked at 4315Å with a 75Å band width (Fig. 12).

The photomultiplier responded to emission from a volume of gas within a solid angle of 10 degrees and 3-inches in length. The length corresponded to the chamber diameter. The angular field of view for the large window was defined by field stops of blackened, drilled brass sheet with the Kistler-mounted sapphire window the stops were formed by the Kistler adapter

structure itself.

At the chamber wall opposite the window, the longitudinal length corresponding to this field was 0.7 inches. With the local velocity of sound in the chamber gas on the order of 3×10^3 ft-sec^{-1}, the time required for a pressure pulse to traverse the photomultiplier field of view was about 3×10^{-5} sec. This represents the minimum pressure-light signal lag that can be resolved for a longitudinal mode, and is about 1/30 the period of a 1000 cps frequency.

The transverse optical arrangement gave a solid viewing angle of about 10°.

An absolute calibration of the several photomultiplier-filter-field stop combinations is difficult to do and was not made because only relative emission intensities were sought in the light measurements. Irradiance levels at the tube varied according to whether OH, CH, or total luminosity measurements were being made because of differences in spectral intensity vs wavelength, filter bandwidth, and filter transmission. The sensitivity or gain of the photomultiplier was adjusted according to which wavelength interval was being monitored so that convenient signal levels were obtained. A Farrand Optical Company adjustable battery power supply enabled the phototube to operate linearly over a wide sensitivity range. Three standard sensitivity levels were selected and set by illuminating the desired photomultiplier-filter combination with a standard lamp through a standard

field stop arrangement, and by adjusting the power supply until the desired DC tube output signal level was obtained.

The pressure and light data for all runs were displayed on a dual-beam Tektronix oscilloscope, either a Model 551 or a Model 555. For nearly all runs, a photographic record of a single sweep was made.

The obvious shortcoming of an oscilloscope record is that only a small fraction of a run can be recorded with high resolution. A small number of runs were completely recorded at 64 inches sec^{-1} on a CEC recording system having flat response to 10,000 cps with an appropriate galvanometer.

Time-averaged spectra were taken of the visible radiation from the gases inside the chamber at stoichiometric O/F ratio (O/F = 10) and at chamber pressures of 50, 100, and 150 psig. An astigmatic Hilger and Watts Raman Spectrograph with quartz optics was used.

The slit of the spectrograph was parallel to the engine axis, and the system was focused so that the image of the 5-1/2 inch clear length of the quartz window (see Fig. 5) just filled the length of the slit.

Spectra at each chamber pressure were photographed on a single Kodak Spectrographic Plate Type III-0. Exposure time was 2 and 4 seconds in all cases. Effective exposure at the plate used a 200 micron slit width at each chamber pressure. The intensity in the chamber usually peaked about 2.5 inches from the injector face. The spectral plate was read at this peak-intensity position by a densitometer to determine density levels

of emission.

As the spectrograph is astigmatic, the spectra are spatially resolved along the engine axis and show the spectrum vs axial length of the chamber over the distance 1.9 inches to 7.4 inches downstream of the injector face. That is, at any wavelength, every point along a vertical line in the spectrogram corresponds to an equivalent point along the chamber length.

III. RESULTS

A. General Remarks

The mode of primary interest here was the fundamental first-harmonic longitudinal mode of 1100 cps. The mode of secondary interest was the first tangential (standing) mode of 7,000 cps (see Ref. 1a). The 14,000 cps first radial mode (Ref. 1a) and 44 and 200 cps longitudinal modes were also observ in the present work but were not studied. The present pressure-time results were very "hashy", and the presence of secondary "modes" could perhaps be extracted from the data. This was not attempted in the present work. The "pops" often observed with the hydrazine-type fuels and N_2O_4 oxidizer were never observed here.

Figure 13 shows typical motion-picture sequences of the luminosity fluctuations occurring in our engine with the gaseous methane-air and the liquid pentane-air systems. Luminous "bundles" move down the motor and then out of the nozzle. This bundle "vibrates" at 1100 cps as it moves down the chamber. The 7000 cps tangential and 14,000 cps radial modes cannot be seen on the film clips since the direction of oscillation is toward and away from the camera.

B. Premixed Gaseous Methane-Air System

Instability in the methane-air system was studied in some detail last yea (see Ref. 4). The main controlling factors were:

1) diameter of injection port circle,

2) chamber pressure,

3) injection velocity, and

4) O/F ratio

This system was re-examined in this year's work with improved instrumentation. The results are discussed below.

1. Pressure Oscillations.

Figure 14 gives oscilloscope traces of the pressure instability and shows the transition from longitudinal (1100 cps) to tangential (7000 cps) instability as a function of chamber pressure and injector velocity. The 150 psig trace also shows the 200 cps mode. Figure 15 gives the instability map. Other instability maps showing the effect of port geometry, etc. were given in Ref. 4.

Figure 16 gives typical pressure traces measured with two Kistler transducers mounted on opposite sides of the motor (2.8 inches downstream from the injector face). The traces were essentially in phase, indicating that a plane pressure wave travels down the motor. This feature is important to the interpretation of pressure-emission measurements described later, which were made by replacing one of the transducers with a phototube.

The amplitude of the 1100 cps was a function of the injection velocity and chamber pressure and ranged between 15 to 35% of the chamber pressure as the injection velocity approached sonic velocity. Figure 17 summarizes the amplitudes observed with various injectors.

The 7000 cps transverse mode is shown in Fig. 18. The two pressure taps are on opposite sides of the motor and the scope traces are 180° out of phase, agreeing with the predictions for transverse mode by the Purdue workers based on organ-pipe arguments. In some cases, the peak-to-peak amplitude was greater than twice the mean chamber pressure. One-half cycle of the 200 cps mode is also evident (also see Fig. 14).

2. Initiation and Dampening.

The pressure-time relation during a complete run was monitored on a CEC recorder since events prior to instability may provide a guide in finding the cause of instability.

The recorder showed that pressure oscillations were present immediately after the ignition pulse started and the ignition characteristics could not be clearly differentiated from the propellant characteristics. However, a short study was made to examine the effect of the igniter on the 1100 cps longitudinal mode.

The initiation of the 1100 mode in a smooth start and also the dampening of this mode in a hard start was observed. Figure 19 gives typical results showing initiation and dampening.

3. Deceleration.

The velocity of the pressure wave was measured using 3 pressure stations positioned along the combustion chamber (4.75, 9 and 13.25 inches from the injector face).

Results (Fig. 20) suggested a deceleration of the 1100 cps pressure wave from about 3300 to 1100 ft/sec (or a multiple thereof) as the wave travelled down the motor toward the nozzle (P_c = 100 psig). An increase in "hash" down the motor is apparent.

4. OH and CH Emission.

In the previous work (Ref. 4), a time delay of 0.1 - 0.2* was observed between the pressure pulse and the accompanying light emission, but results had a limited reproducibility and there was some question in our mind about experimental errors.

The present work used an improved instrumentation and are now limited only by subjective error in comparing the peaks of the "hashy" scope traces of pressure and emission.

The present results essentially are identical to those of last year. Figure 21 gives the pressure trace and the corresponding OH and CH traces for several chamber pressures. A 0.2 millisec delay is evident for both the OH and CH emission in several cases. However, a repeat run at 100 psig chamber pressure (photograph on right) gave essentially a zero delay, indicating a difficulty in reproducibility.

* A 0.3 millisec delay was very occasionally observed (see earlier).

5. Time-Averaged Emission.

Time-averaged emission spectra were investigated in order to determine whether other emission lines (in addition to the above OH and CH lines) appear. Such lines could then perhaps be used to trace the combustion phenomena in the motor.

The spectra consisted of (a) the strong OH and CH lines and also a continuum at 2800 to 4400Å and (b) weak emission lines around 3500Å. Figure 22 gives typical results with the intensity normalized to the 3097Å intensity. The relative intensity of the 4315Å CH line decreased somewhat and the ratio of the continuum to the 3097Å OH intensity increased somewhat with increased chamber pressure, but the relative spectra at 50 and 150 psig are essentially very similar. The continuum presumably is the CO+O continuum.

C. Liquid Pentane-Air

1. Pressure Oscillations.

The main factors controlling instability in the liquid pentane-air system appeared to be mixing and O/F ratio. In general, the pressure oscillations in this system were much "hashier" than the oscillations observed with the gaseous methane-air system.

The 1100 cps longitudinal mode (Fig. 23) was almost always observed. The amplitude of this mode usually was about 25% of the chamber

pressure with impinging jets of fuel and oxidizer and about 15% with non-impinging jets. Figure 24 shows this longitudinal mode over a longer period of time.

A weak transverse mode (Fig. 25) was observed with a stoichiometric system and non-impinging jets in two cases out of five. The transverse mode was observed in all cases with a fuel-rich system (λ = 0.832) at a high chamber pressure (100-150 psig) and with impinging jets. Amplitude was less than 10% of the chamber pressure. A "hard" ignition was tried, but the amplitude still was small.

When the metal chamber was replaced by a Plexiglas chamber of the same dimensions, the engine ran stably. This stability was probably due to ablation of the Plexiglas walls, for ablation has been noted as a "cure" for instability by other workers.

2. Initiation and Dampening.

The "hashy" nature of the CEC-recorded pressure traces (see Fig. 24) prevented a detailed study of this aspect. The initial oscillations were less than 5% of the chamber pressure and some dampening seemed to occur.

3. Deceleration.

Several runs were made in an attempt to record the deceleration of the pressure wave. Unfortunately, the middle pressure station was not recording, and deceleration therefore could not be deduced. The program was ended before the middle station could be repaired.

4. OH, CH, and "Total" Emission.

In all cases, 0.3 to 0.4 millisec time lag was observed between the pressure pulse and all emission peaks. The value of the time lag again was non-reproducible and seemingly was essentially independent of the following parameters:

chamber pressure	-	50 to 150 psig
λ	-	0.83 to 1.4
injector parameters	-	(see earlier)

Figures 26 and 27 give typical results at 100 and 150 psig for an impinging injector and compares the pressure trace with OH, CH, and total emission traces. A 0.3 millisec lag is apparent. Figure 28 gives similar results for a non-impinging injector.

5. Time-Averaged Spectra.

Typical results are given in Figs. 29 to 31 to show the effect of pressure and injector impingement and also the effect of injection velocity. (Figure 29 corresponds to a low injection velocity while Fig. 31 corresponds to a high injection velocity.)

The continuum emission (relative to 3097Å OH emission) increased as the chamber pressure and the injection velocity was increased. Other weak emission lines in the 3500Å range appeared with the higher injection velocity (Fig. 31) and particularly when the fuel and air streams were non-impinging. The CH relative emission appeared to decrease somewhat with increasing pressure. Fig. 32 gives typical raw data (see later).

IV. DISCUSSION

The limited reproducibility in the pressure-time and emission-time traces in the present work seemingly was due to uncontrolled wave phenomena in the motor. A statistical treatment of the results perhaps would extract trends showing a correlation between time delay and motor parameters. However, the intent of this program was to explore the fundamental relations between time delay and motor parameters, and a statistical approach was discarded as being unsatisfactory.

The reasons for the limited reproducibility are not clear, but one might suspect that local turbulent combustion phenomena play a role. If this speculation is correct, emission measurements would be of limited usefulness as a diagnostic technique for studying combustion instability.

The time lags of about 0.2 millisec for methane-air and 0.3 - 0.4 millisec lag for liquid pentane-air measured in this work in general agree with the 0.3 - 0.4 millisec lag of Zucrow (Ref. 1a). The increased lag in the present work with the liquid pentane presumably involves vaporization kinetics. However, the limited reproducibility prevents a detailed analysis of the results.

The apparent decrease in the intensity* of the 4315Å CH emission with an increase in chamber pressure agrees with the results observed with laboratory flames (Ref. 2). The increase in the CO + O emission with

*Relative to the OH emission at 3097Å.

increasing chamber pressure and with non-impinging injectors is puzzling and remains unexplained. Furthermore, this CO + O emission begins to obscure the CH emission at higher chamber pressure so that the CH emission becomes almost useless as a diagnostic indicator of reaction kinetics.

Another result of the present work is the experimental pressure-time data related to the initiation and dampening of the 1100 cps longitudinal mode. Unfortunately, this phase of the present work was started late in the program and could not be pursued in detail.

Fig. 32 gave typical raw spectral data for the methane-air and pentane-air systems. The time-averaged spectral data include tungsten emission data which could be used to calibrate the plate and thereby convert the "relative" intensities in Figs. 29-31 to absolute intensities. However, this conversion is time-consuming and was not done here in view of the limited reproducibility.

In conclusion, the present results do demonstrate that emission measurements can be made with laboratory engines. However, the results had poor reproducibility and the applicability of emission measurements to large engines is limited by the CO + O continuum and also limited by the greater optical depth of large engines.

V. ACKNOWLEDGEMENTS

Experimental work was conducted by Mr. J. Traylor. Equipment was designed by Mr. B. Dawson and constructed by Mr. Traylor.

VI. REFERENCES

1. For example:

   (a) M. J. Zucrow, J. R. Osborne, and A. C. Pinchak, ARS Journal 12, 758 (1960).

   (b) E. K. Bastress and A. C. Tobey, AFOSR Combined Contractors' Meeting on Combustion Dynamics Research, June, 1965.

   (c) M. J. Zucrow, et al, AFOSR Combined Contractors' Meeting on Combustion Dynamics Research, June, 1965.

2. For example: J. Diedericksen and H. G. Wolfhard, Proc. Roy. Soc. 236A, 89 (1956).

3. J. R. Osborn and R. L. Derr, An Experimental Investigation of Longitudinal Combustion Pressure Oscillations, Purdue Univ., Report No. I-62-8, Aug. 1962.

4. B. Hornstein "Research Study of Light Emission Caused by Pressure Fluctuations in Rocket Engines, Thiokol Chem. Corp., Reaction Motors Div., Rept. No. 5516-F, May, 1965.

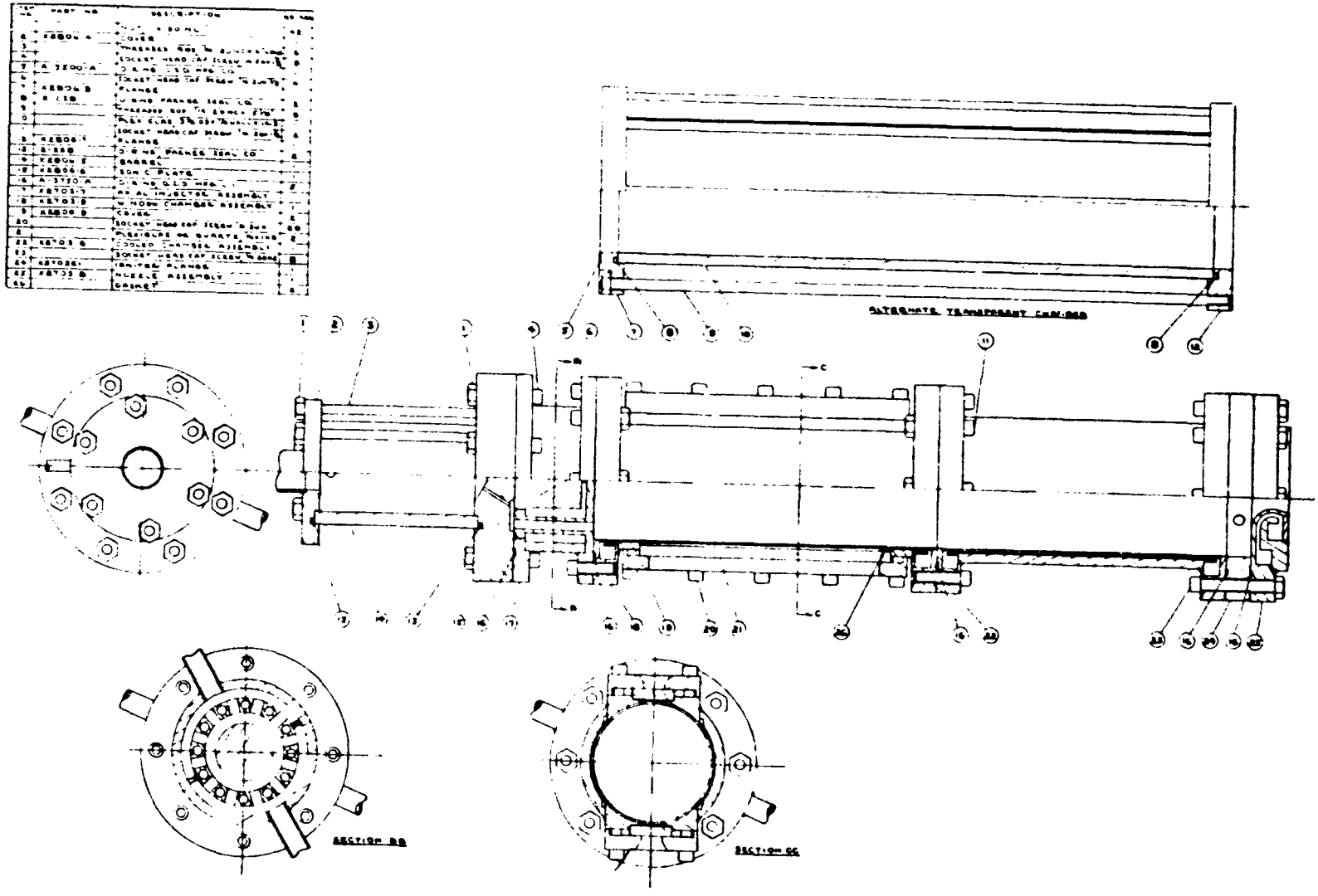

Fig. 1. Assembly Drawing of Basic Engine.

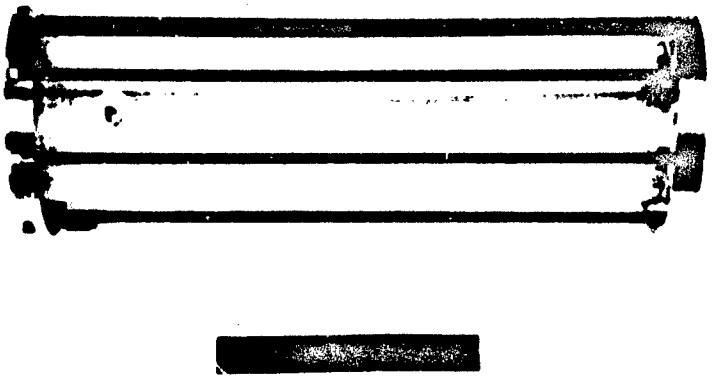

RMD Photo No. 5520-4

Fig. 2. Plexiglas Chamber.

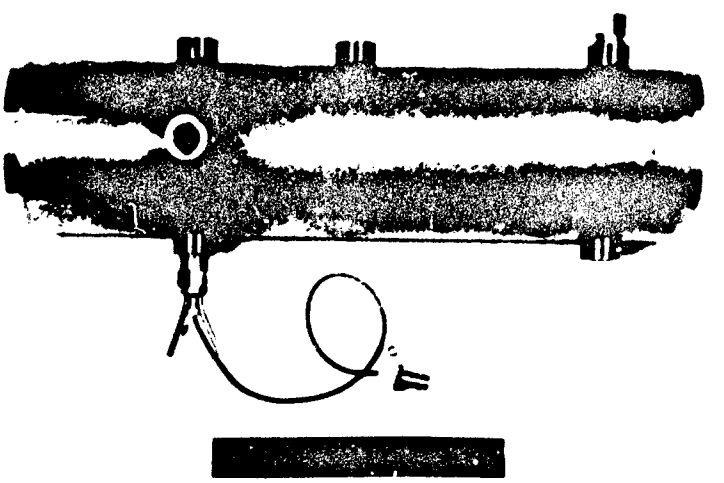

RMD Photo No. 5520-3

Fig. 3. Uncooled Metal Chamber, with Kistler Assembly and Blank Plug.

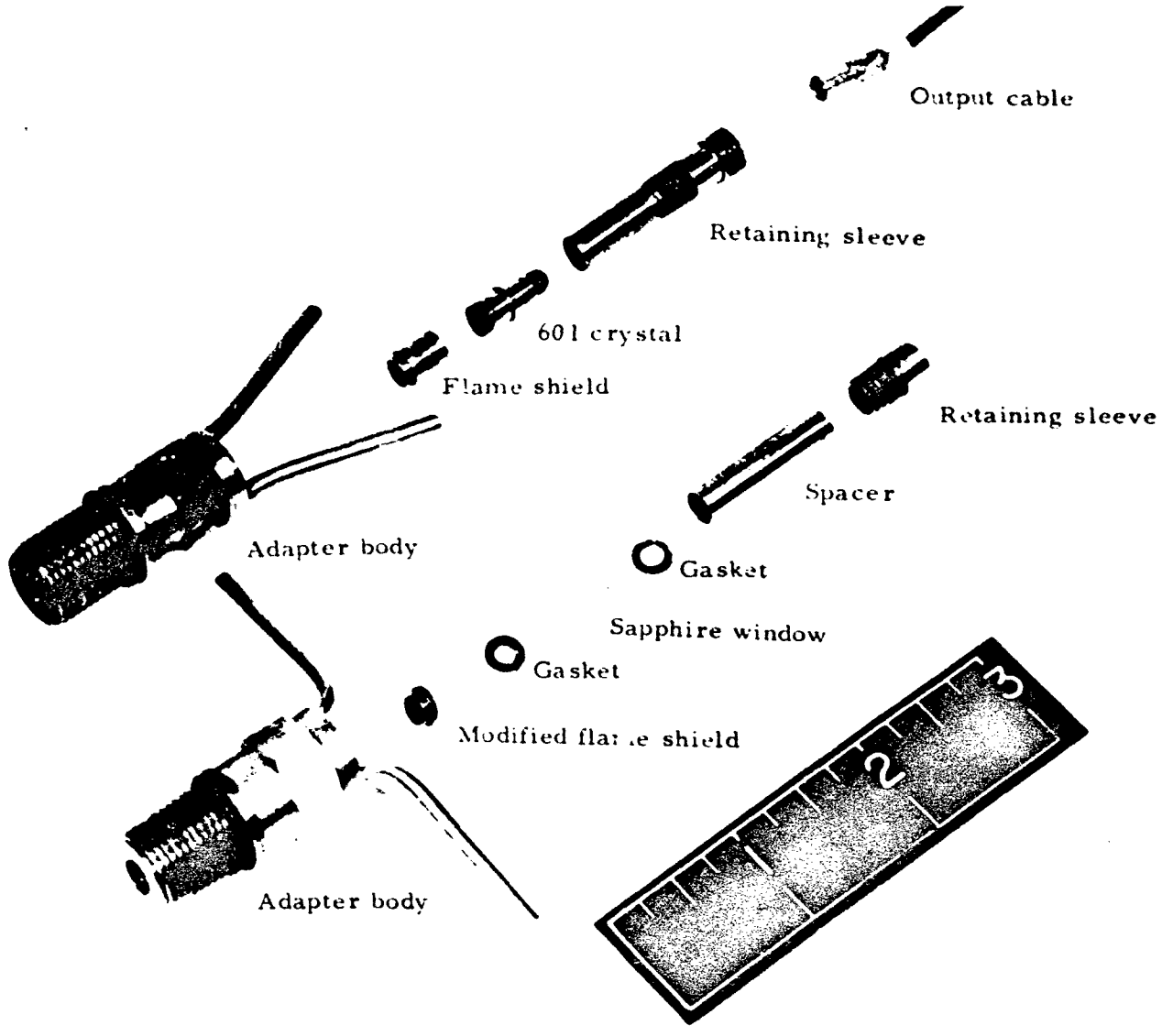

5520-2

Fig. 4. Kistler Pressure Adapter and Window Modification.

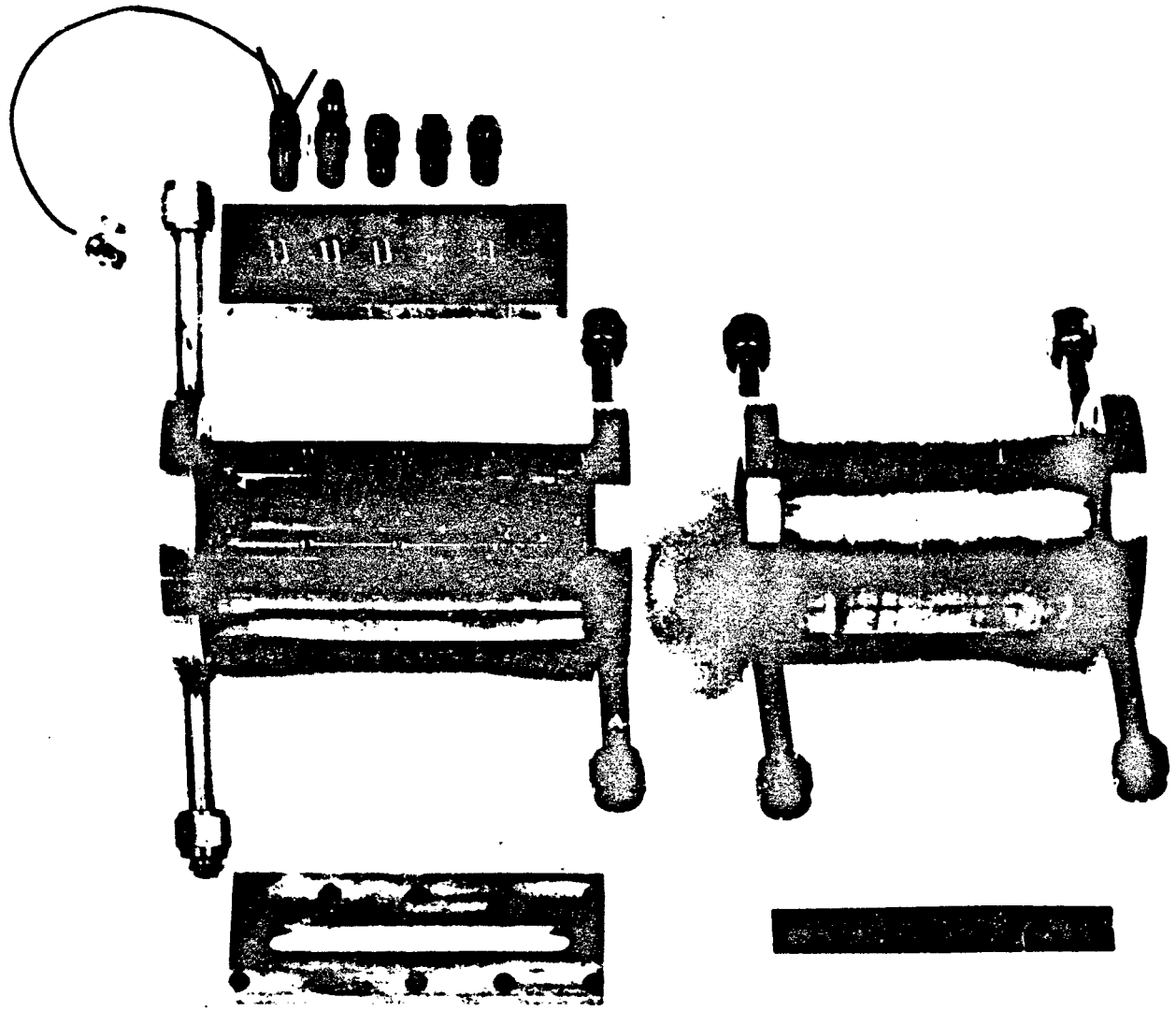

5520-1

Fig. 5. Quartz Window and Pressure Tap Plate.

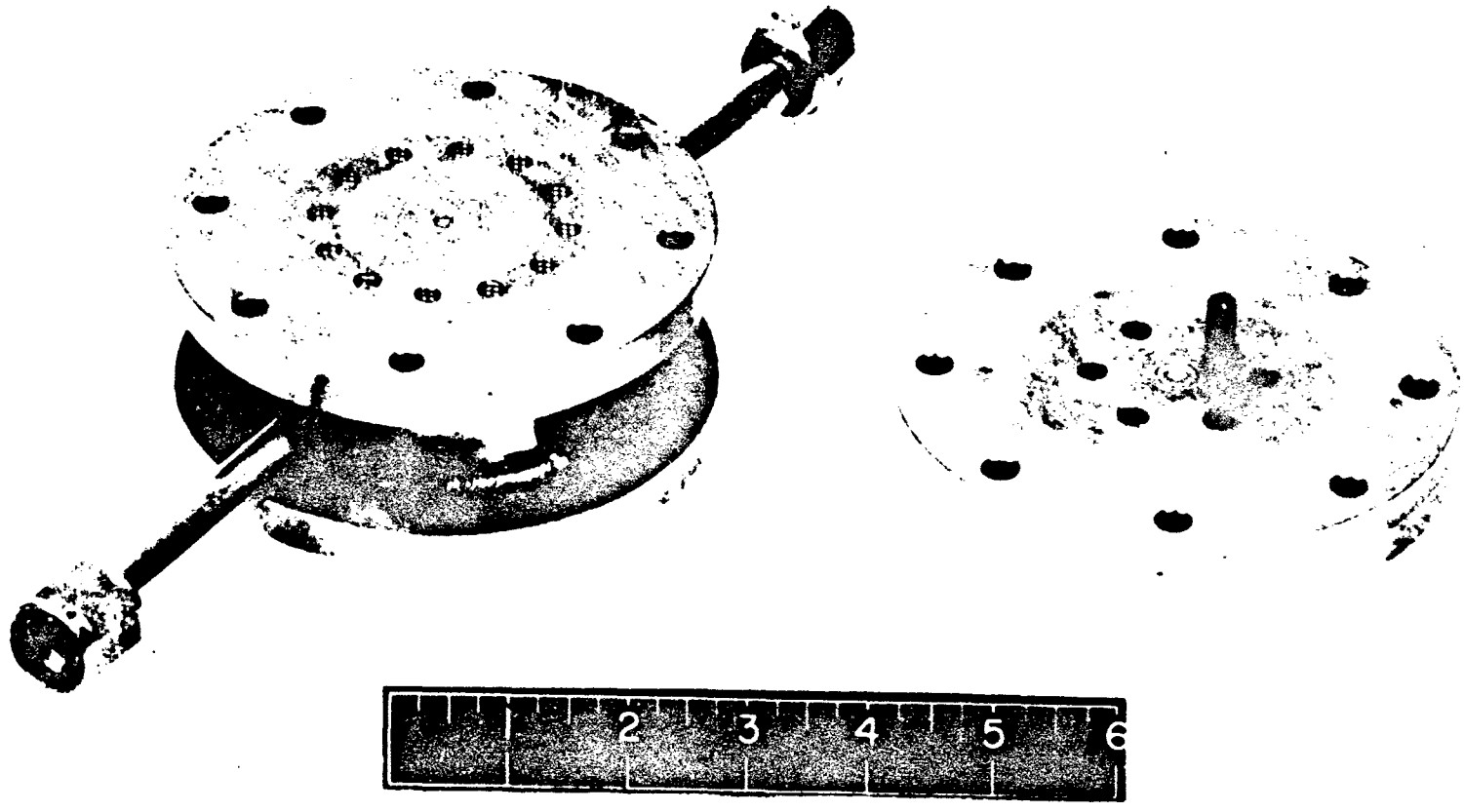

5520-5

Fig. 6. Water-Cooled 12-Port Injector and Uncooled 6-Port Injector for Methane-Air. Note that One Insert is Partially Unscrewed.

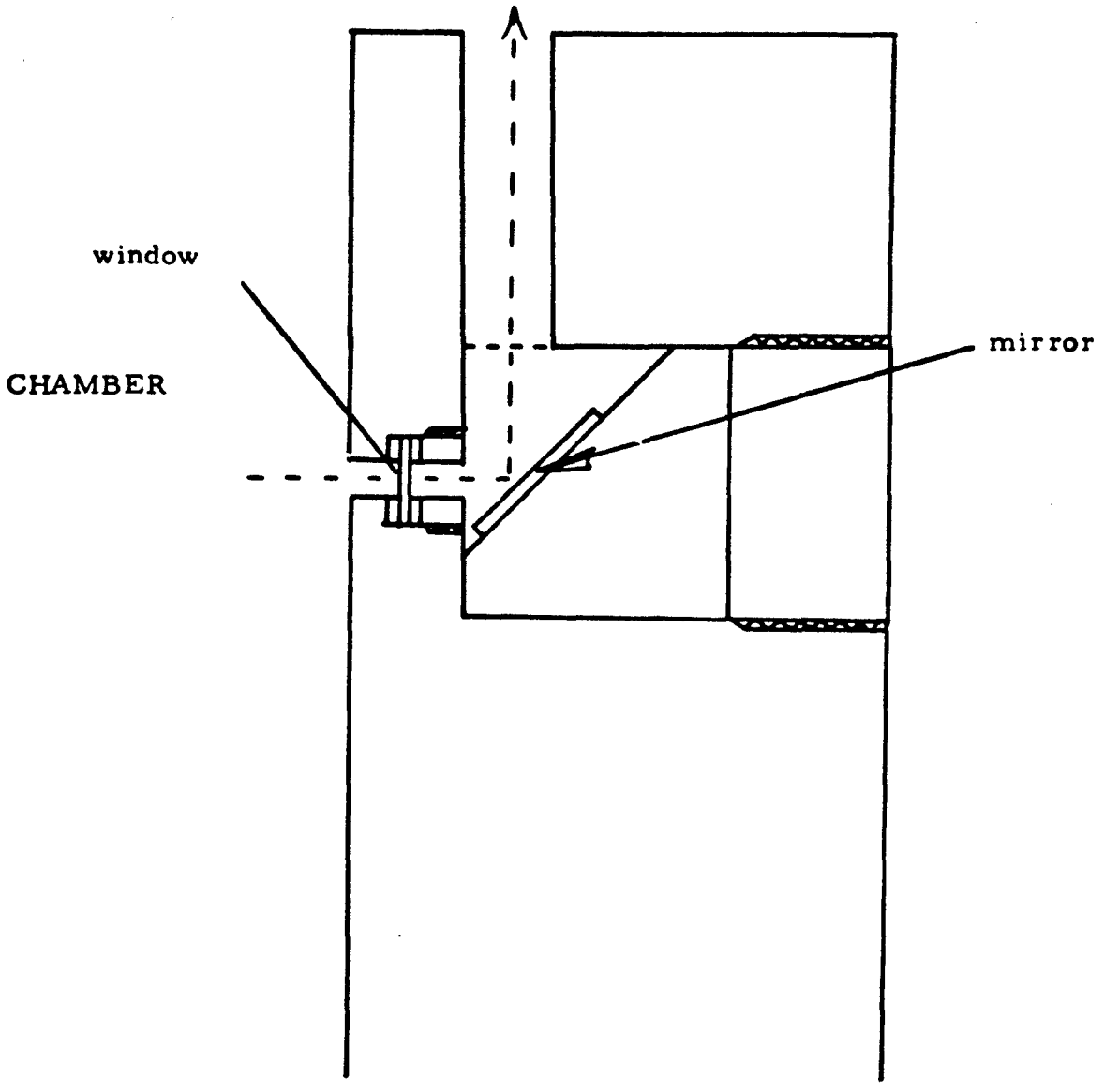

Fig. 7. Mirror Port in Injector to View Transverse Mode.

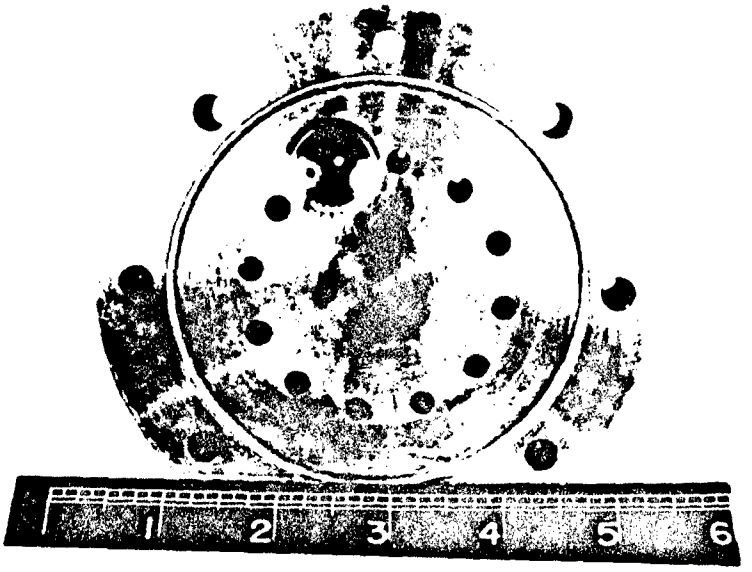

RMD Photo No. 5520-6

Fig. 8. Methane-[illegible] Injector With Mirror Port.

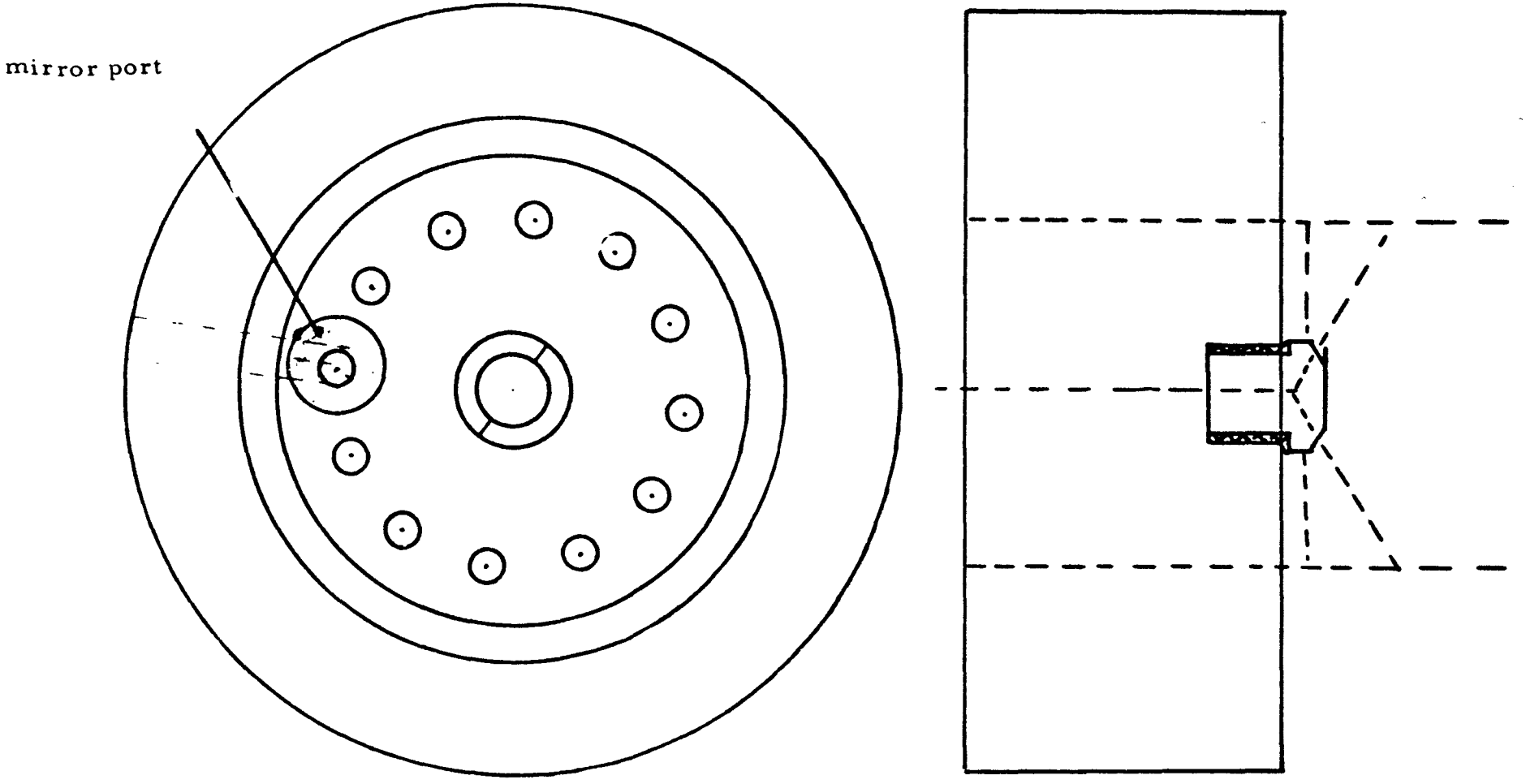

Fig. 9. Liquid Pentane-Air Injector.

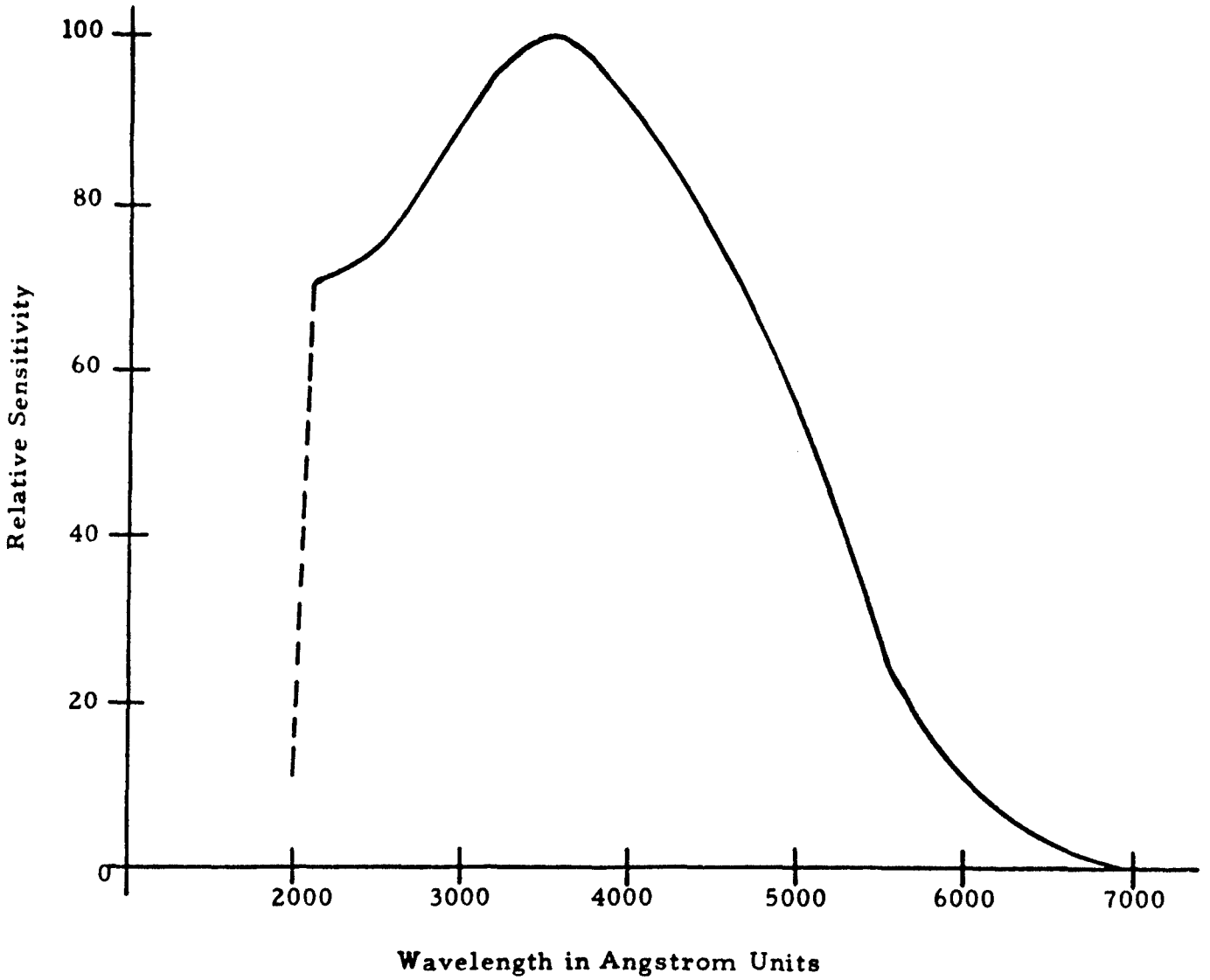

Fig. 10. Spectral Response of RCA Type 1P28 Photomultiplier Tube.

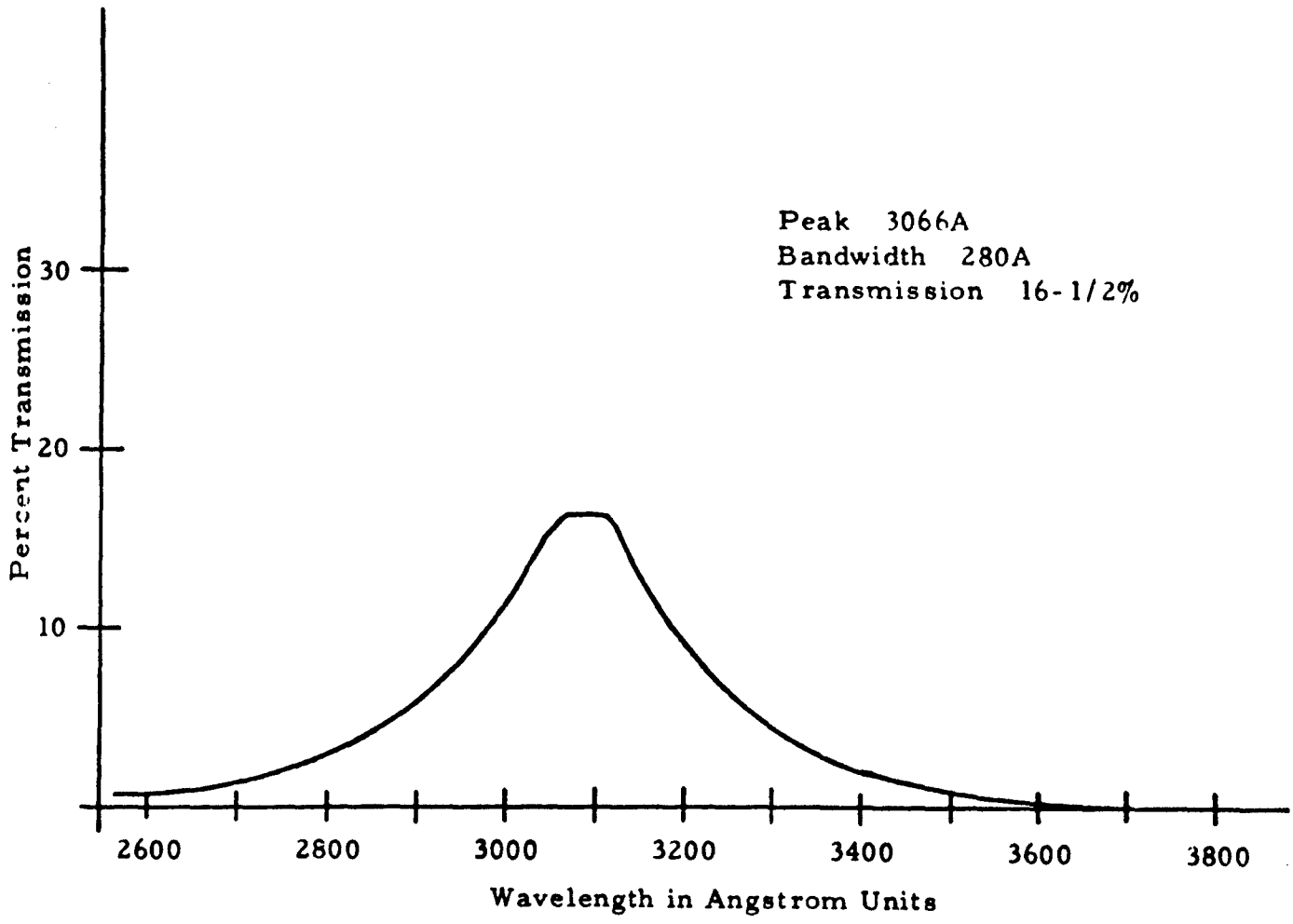

Fig. 11. Transmission of Baird Atomic Interference Filter for OH (0, 0) Band at 3064 Å

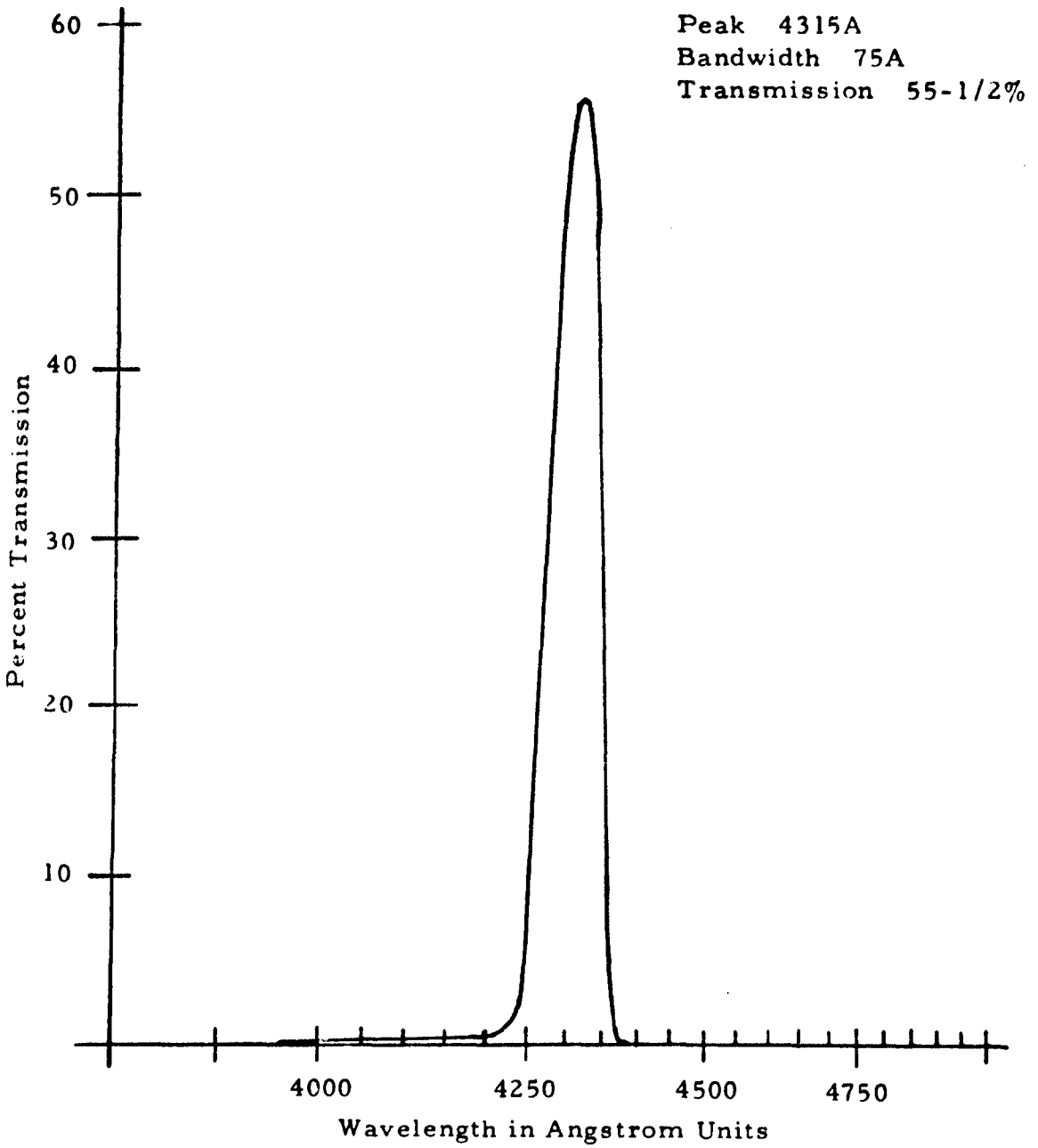

Fig. 12. Transmission of Baird Atomic Interference Filter for CH (0, 0) Band at 4315Å.

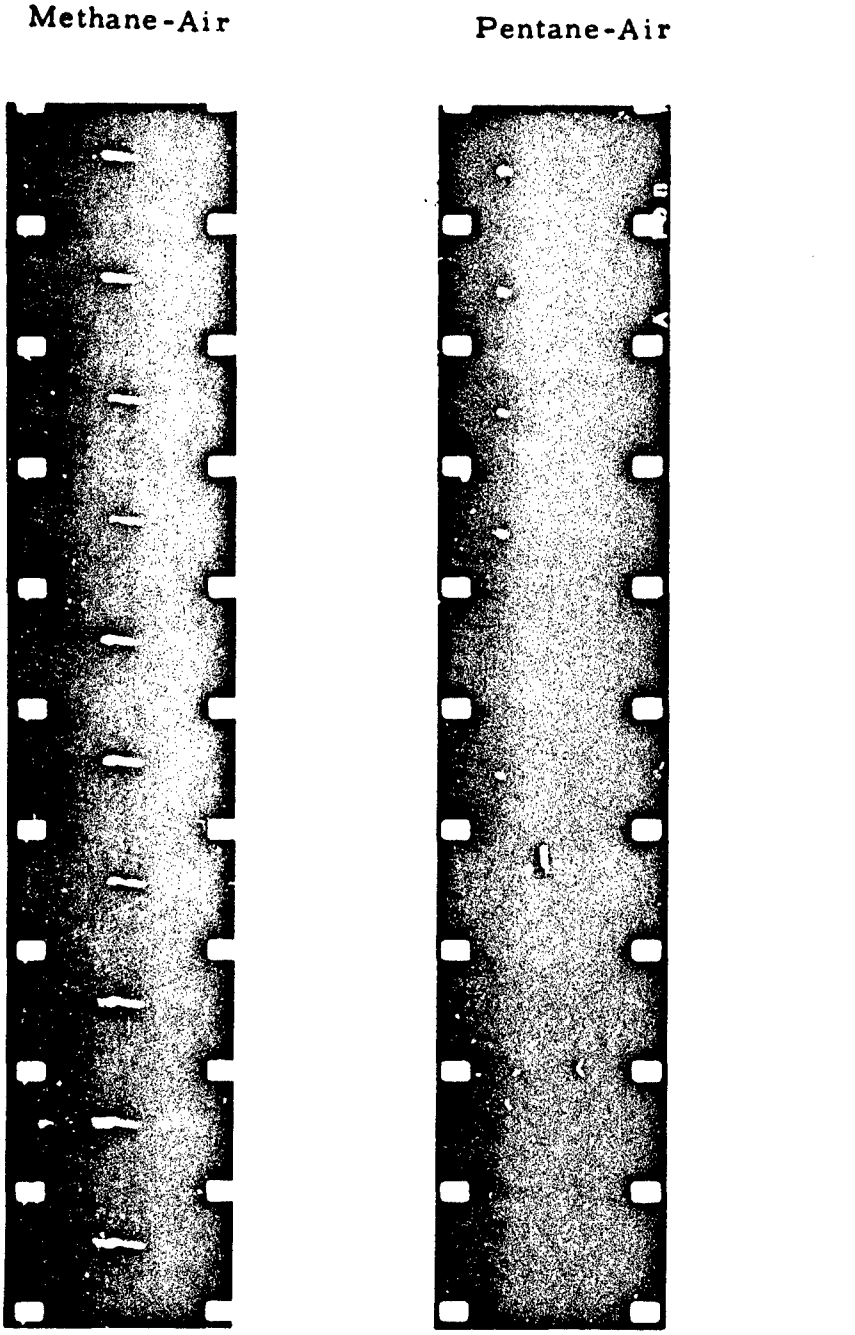

Fig. 13. Typical Motion Pictures of Luminosity in Methane-Air and Liquid Pentane-Air Systems. (4,000 frames/sec)

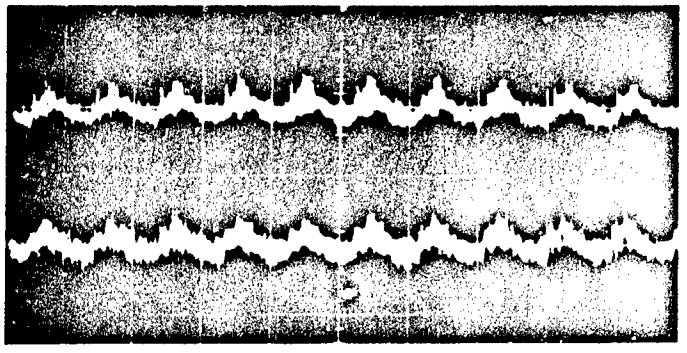

P_c = 50 psig
1100 cps longitudinal

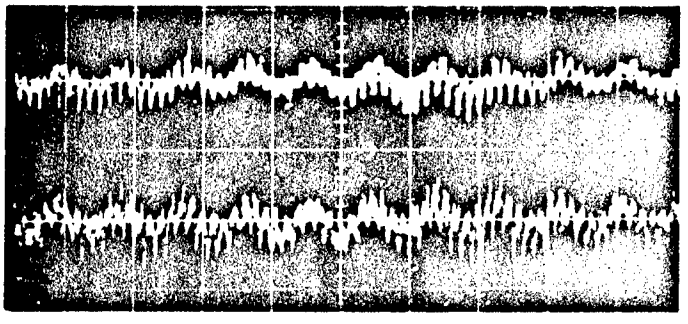

P_c = 100 psig
1100 cps longitudinal
with
7100 cps tangential

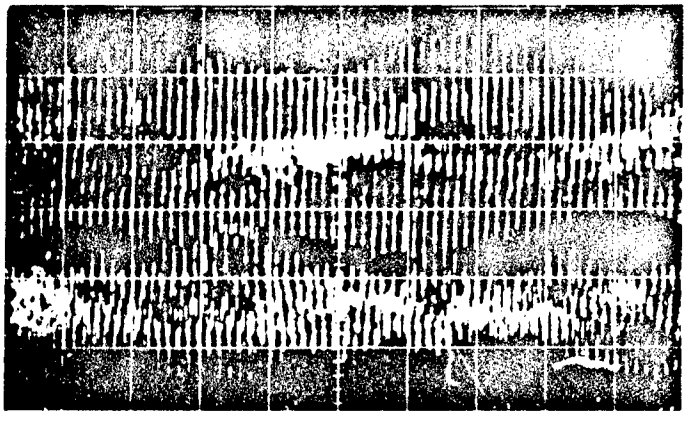

P_c = 150 psig
7100 cps tangential

Fig. 14. Transition from Longitudinal to Tangential Mode with Methane-Air.

Scale: vertical = 25 psi/cm
horizontal = 1 millisec/cm
Injector: 11x0.070

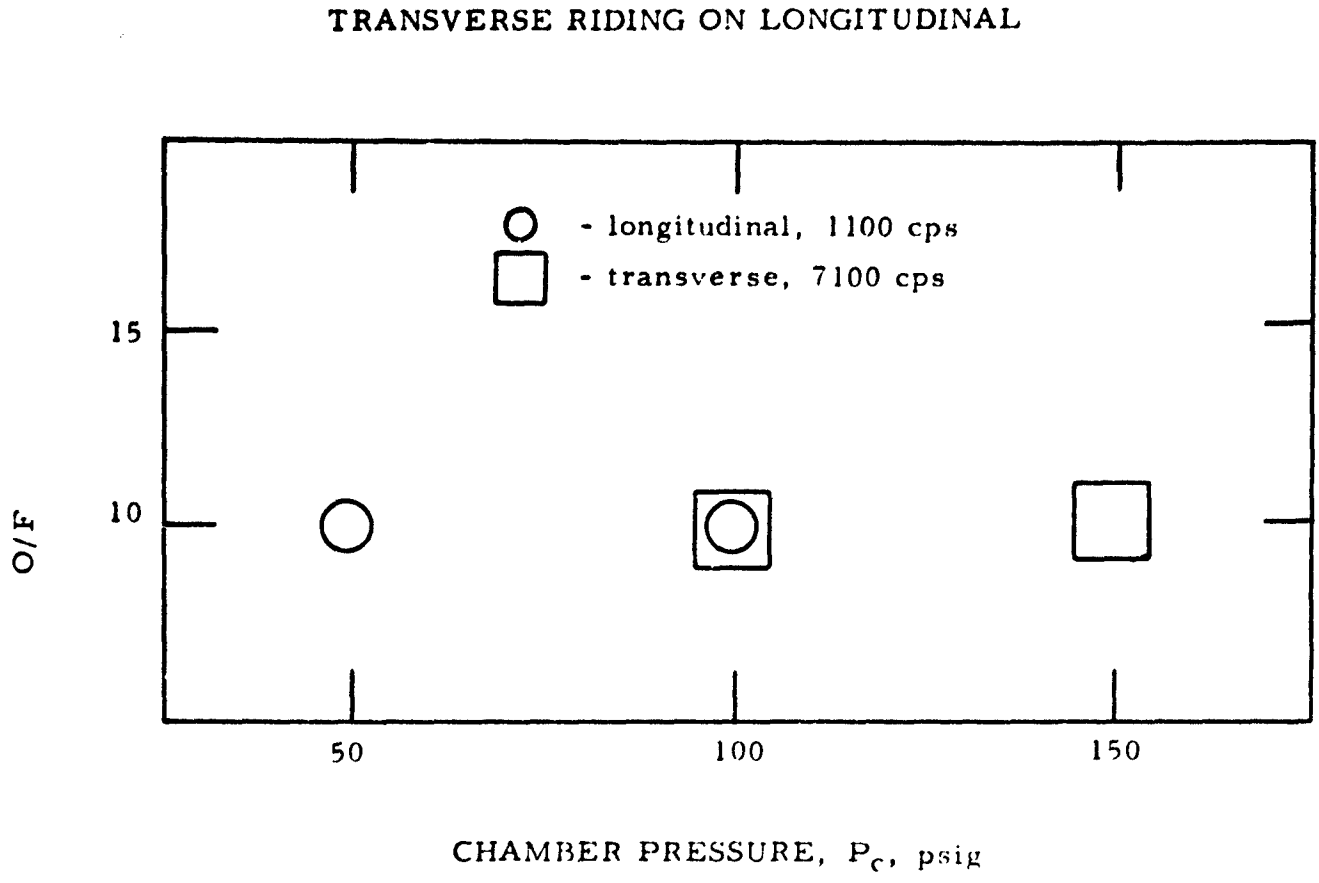

Fig. 15. Typical Instability Map for Methane-Air.

Injector: 11x0.070

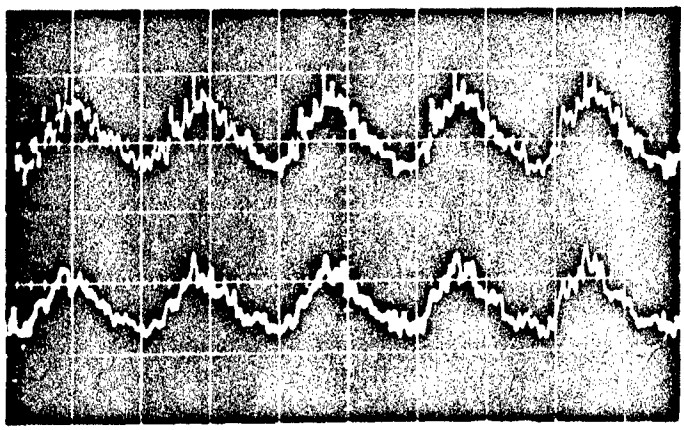

Fig. 16. Evidence for Plane Longitudinal Wave with Methane-Air. (P_c = 50 psig)

NOTE: the two pressure traces are on opposite sides of motor 2.8 in. from injector face.

Scale: vertical = 6 psi/cm
horizontal = 0.5 millisec/cm

Injector: 6x0.100

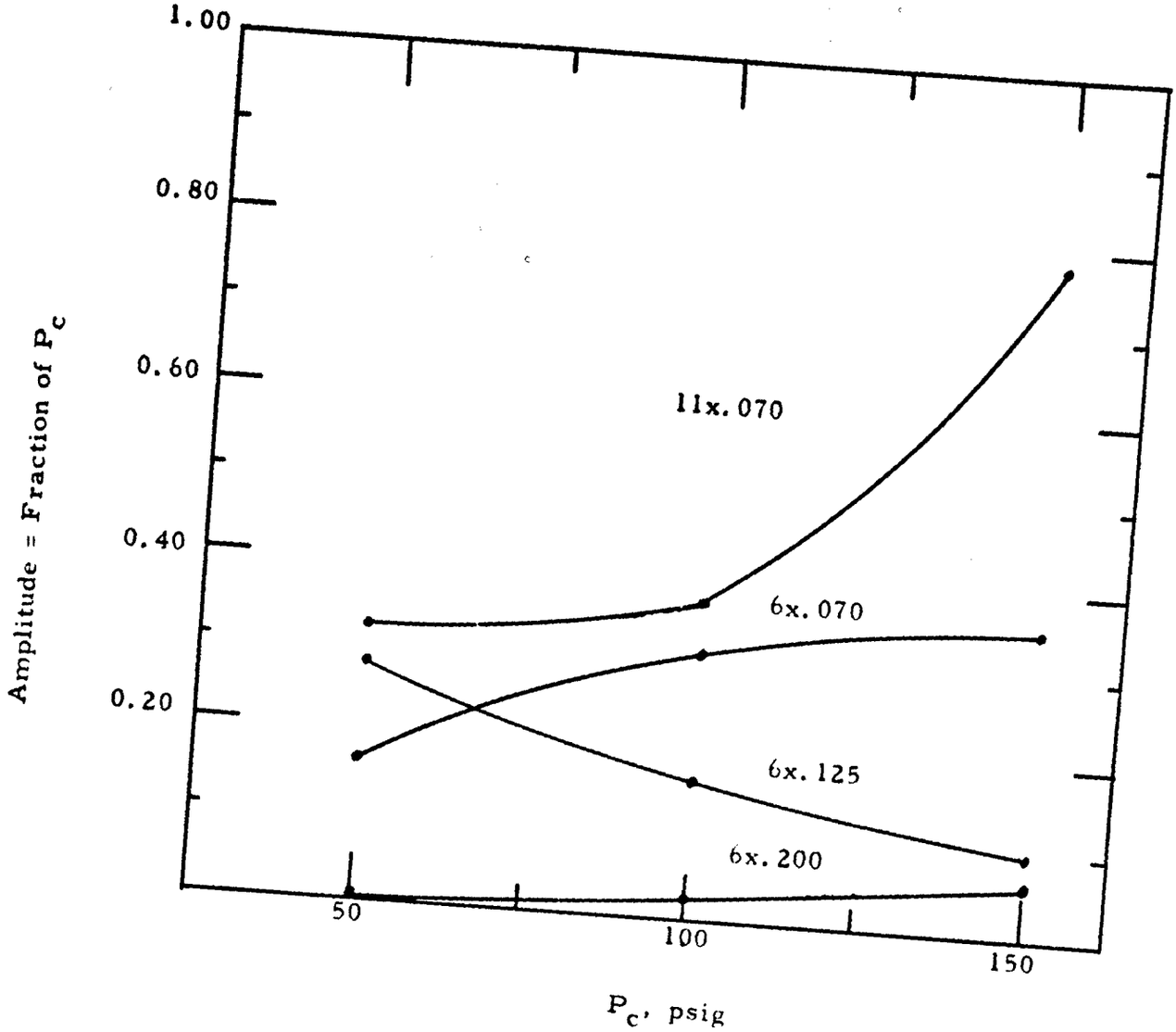

Fig. 17. Amplitude of Instability Mode vs. Chamber Pressure fc - Various Injector Configurations with Methane-Air.

NOTE: 1) Fractional P_c values are averages with highest and lowest experimental values discarded.

2) 11 x 0.070 ~7100 cps tangential mode
6 x etc. ~1100 cps longitudinal mode

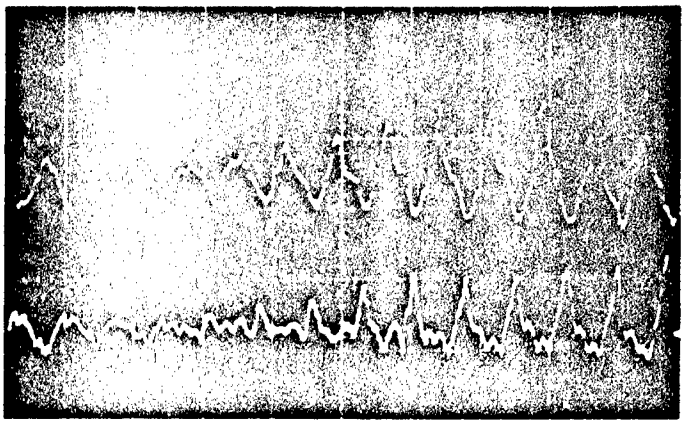

Fig. 18. Transverse Mode with Methane-Air. (P_c = 150 psig)

NOTE: the two pressure traces are on opposite sides of motor 2.8 in. from injector face

Scale: vertical = 100 psi/cm
horizontal = 0.2 millisec/cm

Injector: 11x0.070

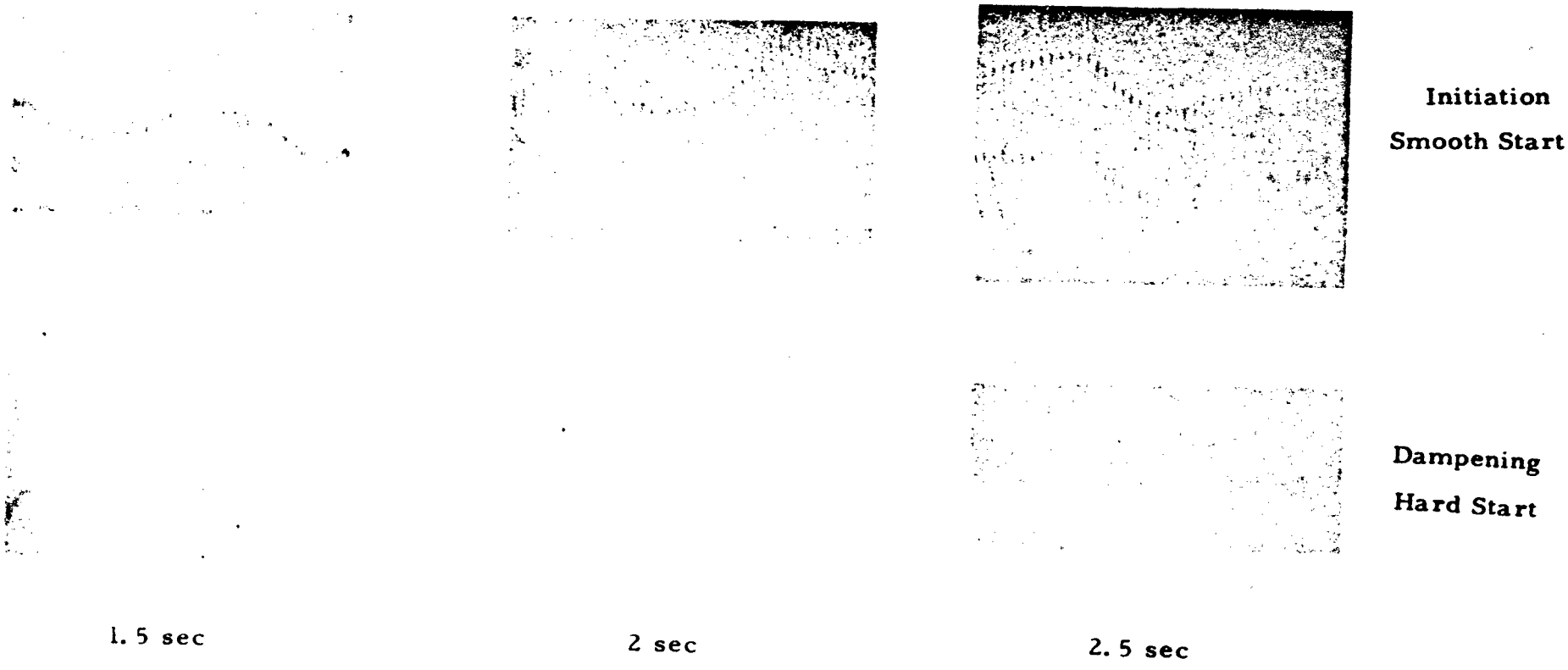

Fig. 19. Initiation and Dampening of Longitudinal Mode with Methane-Air. (P_c = 50 psig)

NOTE: Smooth start: H_2 = 400 psig, Air = 300 psig
Hard start: H_2 = 500 psig, Air = 500 psig
Time = from start of igniter flow.

Vertical Scale: 7 psi/inch
Injector: 6x0.100

Measuring Station
(from injector)

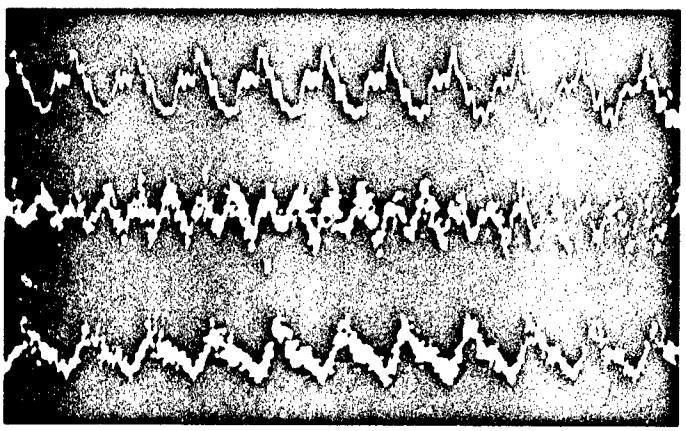

4. 75 in.

9. 0 in.

13, 25 in.

Fig. 20. Decceleration of Longitudinal Mode with Methane-Air. (P_c = 100 psig)

Scale: vertical = 23 psi/cm
horizontal = 1 millisec/cm

P_c (psig

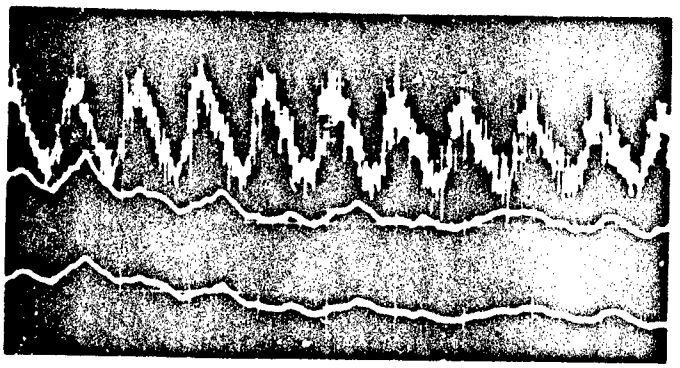

50

vert. = 12 psi/cm; horiz. = 1 msec/cm

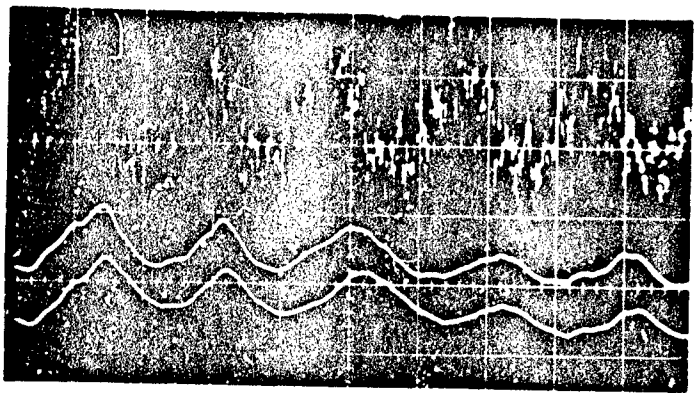

vert. = 12 psi/cm; horiz. = 0.5 msec/cm

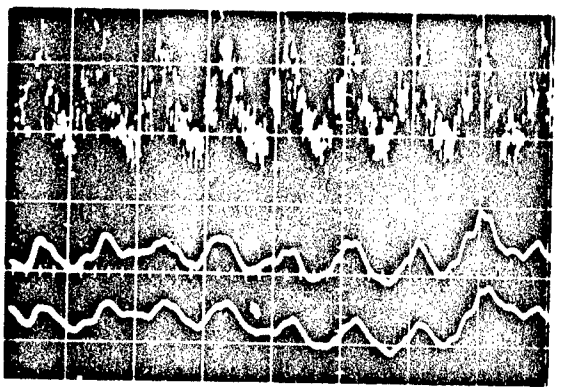

10

vert. = 12 psi/cm; horiz. = 1 msec/cm

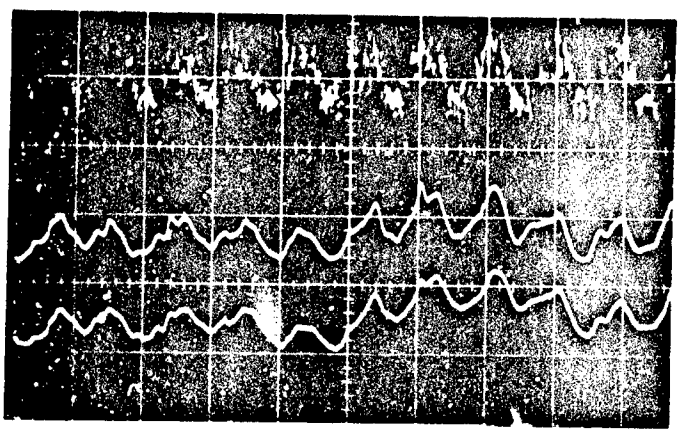

150

vert. = 23 psi/cm; horiz. = 1 msec/cm

Fig. 21. OH and CH Emission Lag with Methane-Air. Reproducibility and Effect of P_c.

Injector: 6x0.100

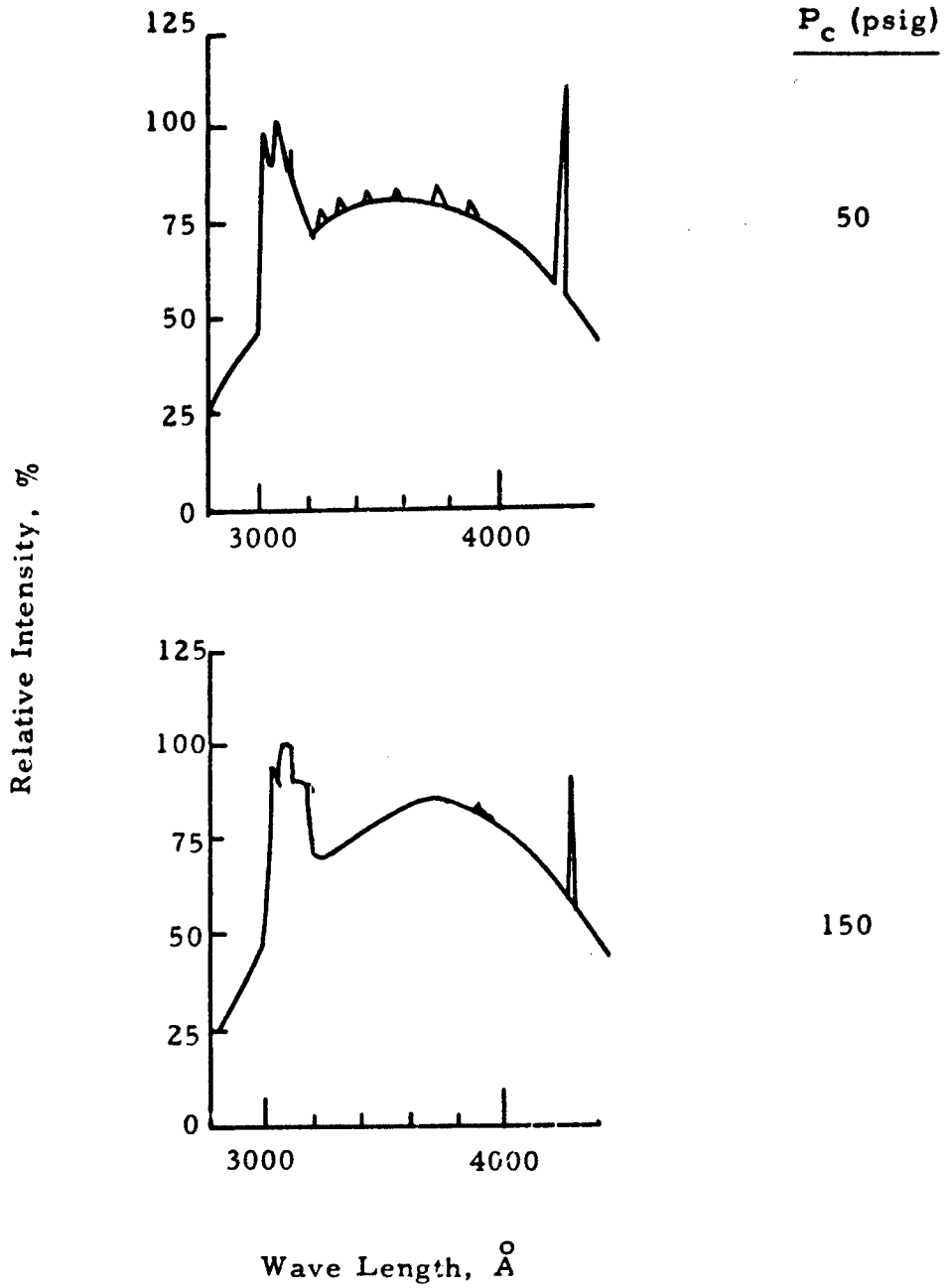

Fig. 22. Time-Averaged Emission Spectra of Methane -Air.

Injector: 6x0.125

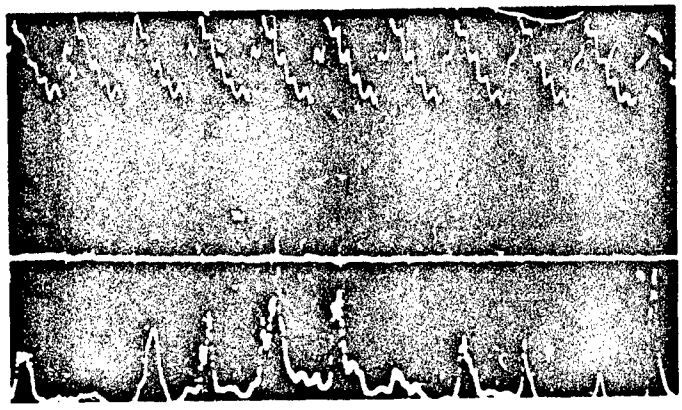

Fig. 23. Typical Oscilloscope Trace of Longitudinal Mode with Pentane-Air.
(P_c = 100 psig)
Pressure Scale: vertical = 28 psi/cm
horizontal = 1 millisec/cm

Injector: fuel = 6x90° impinging
air = 6x0.125

Fig. 24. Typical CEC Trace of Longitudinal Mode After One Second Running Time With O_2-Rich Pentane-Air. (P_c = 150 psig; λ = 1.4)

Scale: vertical = 7 psi/inch
horizontal = 64 in/sec

Injector: fuel = 6x90° impinging
air = 11x0.070

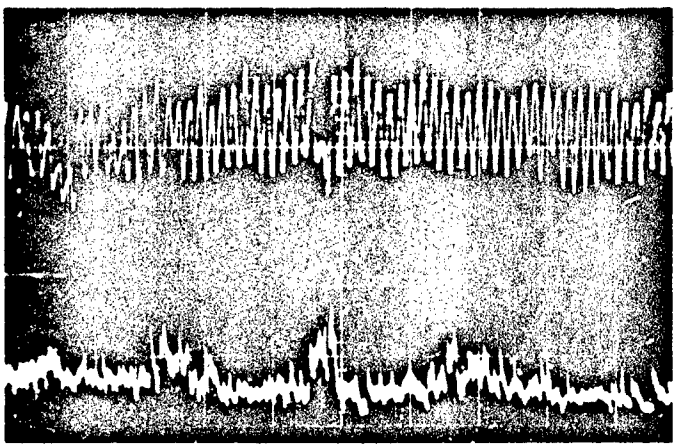

Fig. 25. Transverse Mode with Fuel-Rich Pentane-Air. (P_c = 100 psig, λ -

Scale: vertical = 6 psi/cm
horizontal = 1 millisec/cm

Injector: fuel = 6x90° impinging
air = 11x0.070

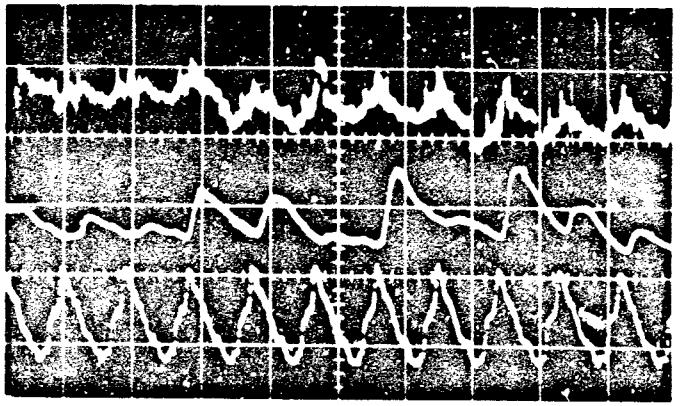

P_c

OH

P_c

vert. = 24 psi/cm; horiz. = 1 msec/cm

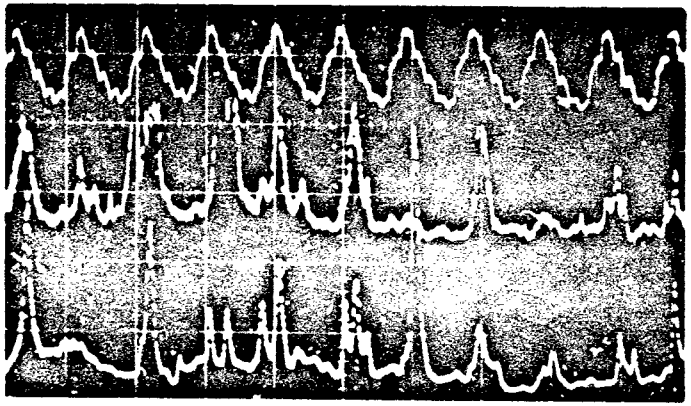

P_c

OH

OH

vert. = 28 psi/cm; horiz. = 1 msec/cm

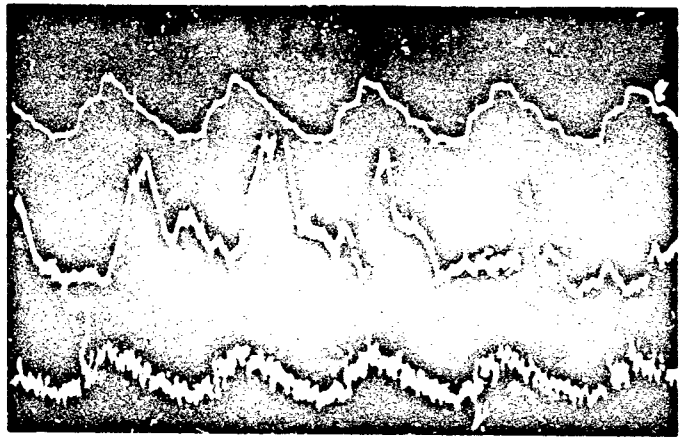

P_c

CH

P_c

vert. =20 psi/cm; horiz. = 0.5 msec/cm

Fig. 26. OH and CH Emission Lag with Impinging Pentane-Air. (P_c = 100 psig)

Injector: fuel = 6x90° impinging
air = 6x0.125

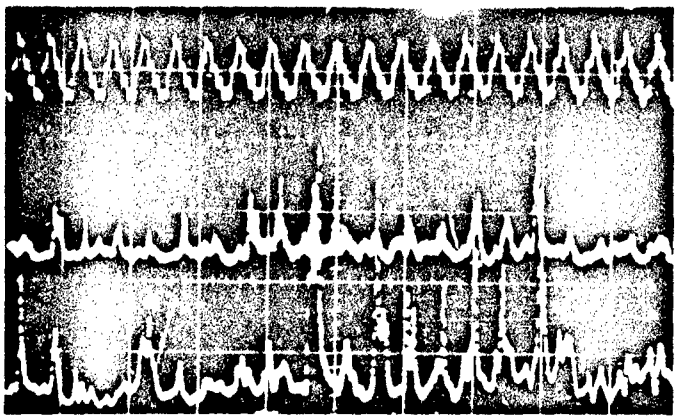

vert. = 28 psi/cm; horiz. = 2 msec/cm.

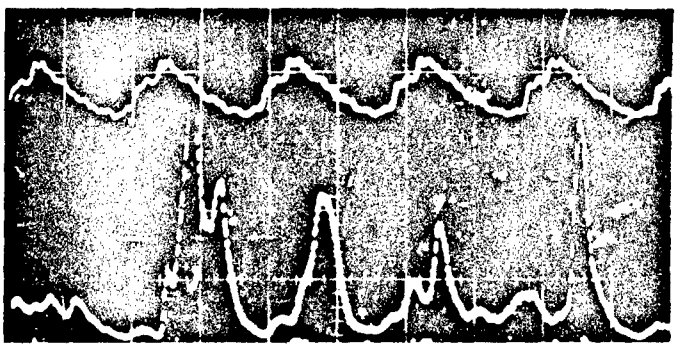

vert. = 14 psi/cm; horiz. = 0.5 msec/cm

Fig. 27. OH and CH Emission Lag with Impinging Pentane-Air. (P_c = 100 psig).

Injector: Fuel = 6x90° impinging
Air = 6x0.125

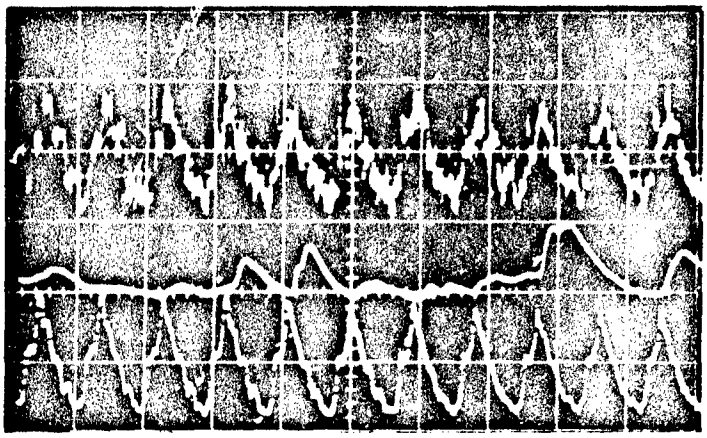

P_c

OH

P_c

3. OH and CH Emission Lag with Non-Impinging Pentane-Air. (P_c = 150 psig)

Scale: vertical = 20 psi/cm
horizontal = 1 millisec/cm

Injector: fuel = 6x90° non-impinging
air = 6x0.125

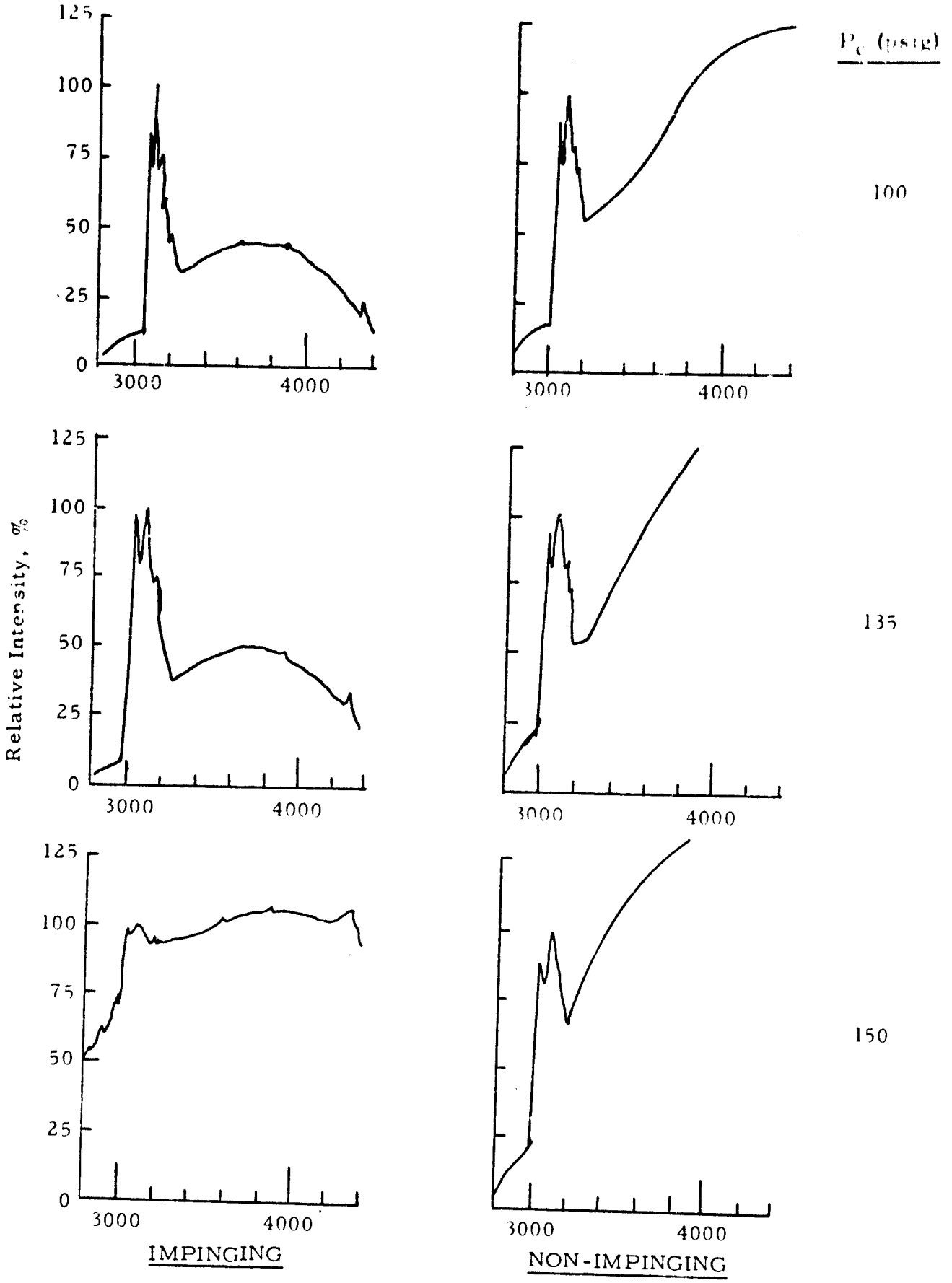

Fig. 29. Time-Averaged Spectra with Pentane-Air. Effect of Impingement and Chamber Pressure on Relative Intensity.

Injector: fuel = 6 x 90°
air = 6 x 0.200

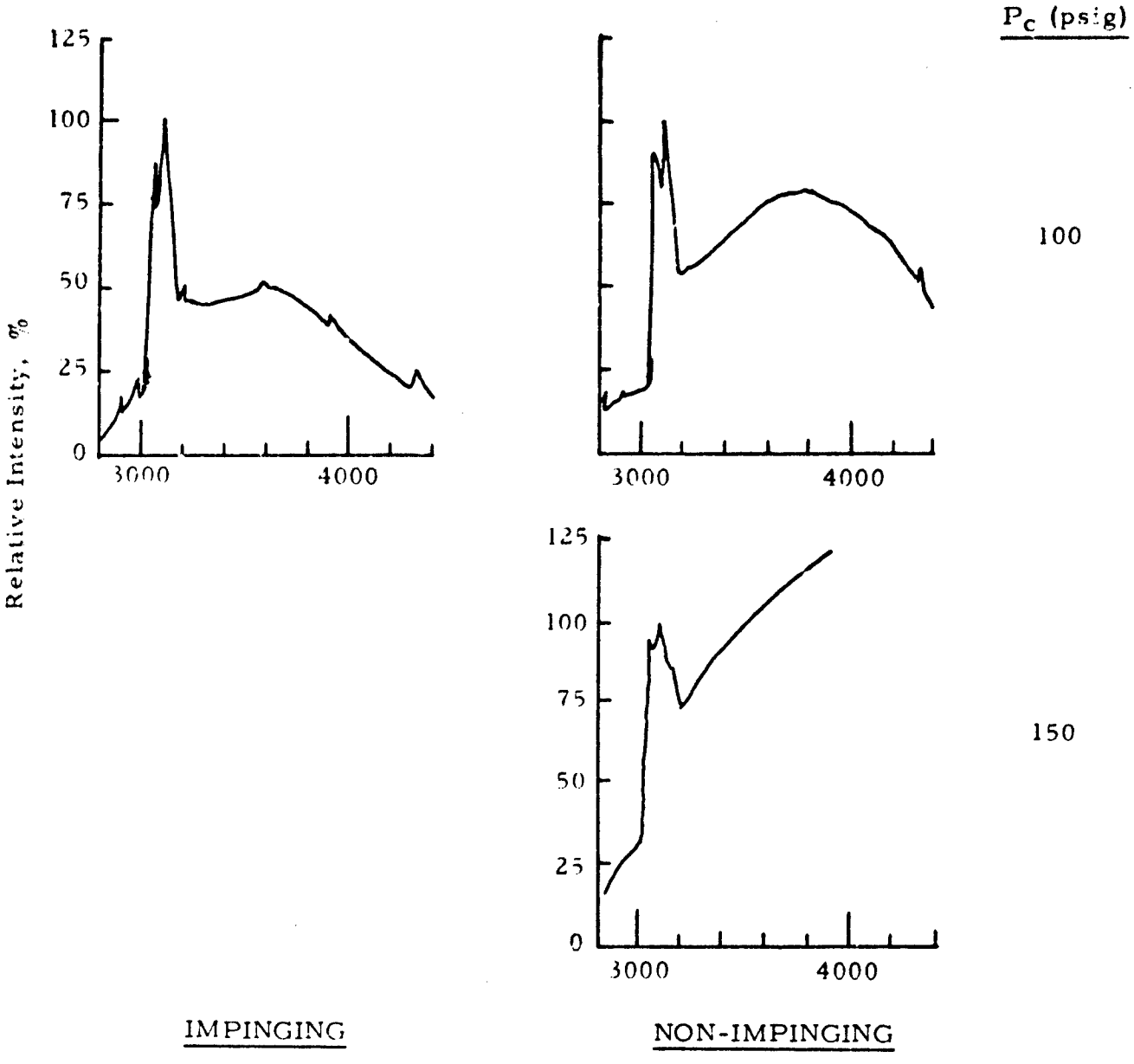

30. Time-Averaged Spectra with Pentane-Air. Effect of Impingement and Chamber Pressure on Relative Intensity.

Injector: fuel = 6 x 90°
air = 6 x 0.125

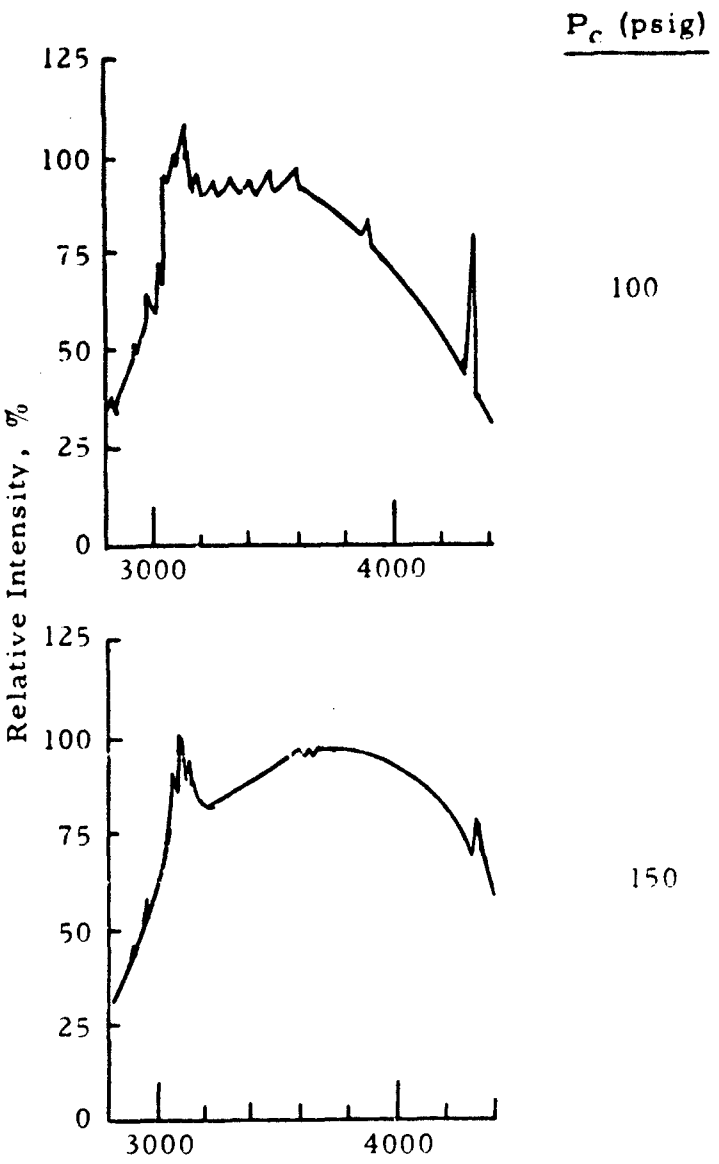

Fig. 31. Time-Averaged Spectra with Pentane-Air. Effect of Impingement and Chamber Pressure on Relative Intensity.

Injector: fuel = 6 x 90°, impinging
air = 6 x 0.100

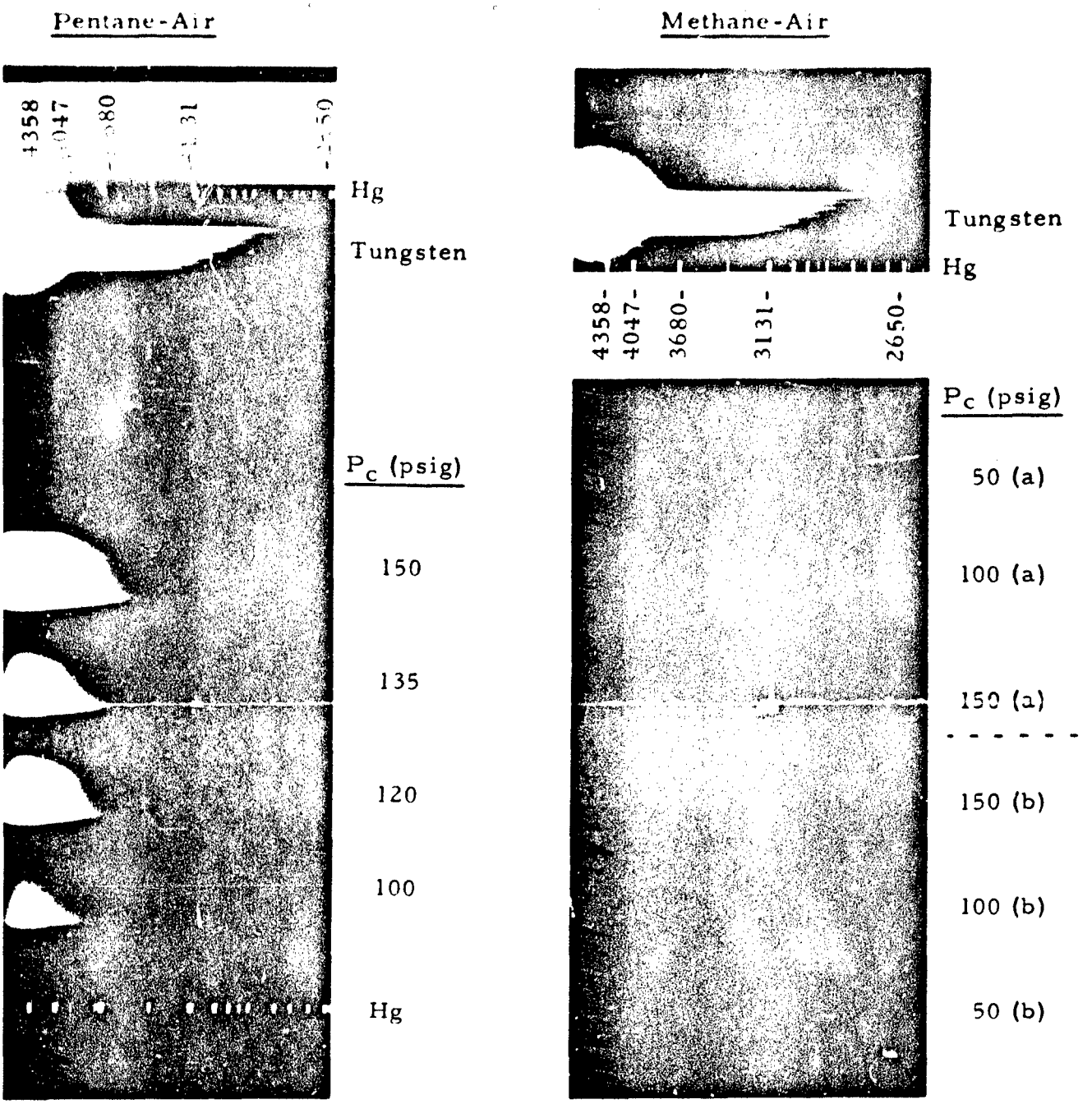

or: fuel = 90° nonimpinging
air = 6 x 0.200

injectors: (a) = 6 x 0.125
(b) = 6 x 0.200

Fig. 32. Typical Raw Time-Averaged Spectra with Methane-Air and Pentane-Air.

film = Kodak UV Plate III-0, 2 sec. exposure
slit width = 200 microns

Unclassified

Security Classification

DOCUMENT CONTROL DATA - R&D

(Security classification of title, body of abstract and indexing annotation must be entered when the overall report is classified)

ORIGINATING ACTIVITY (Corporate author)	2a REPORT SECURITY CLASSIFICATION
Thiokol Chemical Corporation Reaction Motors Division Denville, New Jersey 07834	Unclassified 2b GROUP

REPORT TITLE

Research Study of Light Emission Caused by Pressure Fluctuations in Rocket Engines

DESCRIPTIVE NOTES (Type of report and inclusive dates)

Final Report - 1/1/65-12/31/65

AUTHOR(S) (Last name, first name, initial)

Hornstein, B., Budnik, C., and Courtney, W. G.

REPORT DATE	7a TOTAL NO OF PAGES	7b NO OF REFS
March 1966	64 63	4

CONTRACT OR GRANT NO	9a ORIGINATOR'S REPORT NUMBER(S)
AF 49(638)-1505 PROJECT NO 9711-01 [redacted] 61445014	5520-F
	9b OTHER REPORT NO(S) (Any other numbers that may be assigned this report) AFOSR 66-0779

AVAILABILITY/LIMITATION NOTICES

[redacted]

SUPPLEMENTARY NOTES	12 SPONSORING MILITARY ACTIVITY (SREP)
	Air Force Office of Scientific Research Washington, D. C. 20333

ABSTRACT

This program was to investigate the usefulness of spectroscopy as a diagnostic technique for studying combustion instability in a rocket chamber. Main emphasis was given to investigating pressure and the 3064Å (OH) and 3154Å (CH) emission as a function of time in order to study the time lag between pressure and emission. The 1100 cps longitudinal mode and the 7100 cps tangential mode in a cylindrical motor 3 inches in diameter and 16 inches long were investigated. Two propellant systems were used, a premixed methane-air gaseous system and a liquid pentane-gaseous air system.

Optical results were limited in reproducibility, perhaps because of local turbulent combustion phenomena. Time-averaged spectra indicated no other strong spectral lines in the 2800-4400Å range but did indicate that a CO + O continuum existed and became more intense as the chamber pressure increased and particularly when non-impinging jet injectors were used with pentane-air system. This intense CO + O continuum obscures the CH emission and severely limits the usefulness of spectroscopy as a diagnostic tool. The initiation and dampening of the 1100 cps longitudinal mode was briefly studied.

D FORM 1 JAN 64 1473

Unclassified

Security Classification

14. KEY WORDS	LINK A		LINK B		LINK C	
	ROLE	WT	ROLE	WT	ROLE	WT
Combustion Instability						
Longitudinal Mode						
Transverse Mode						
Methane-Air Combustion						
Propane-Air Combustion						
Spectroscopy						

INSTRUCTIONS

1. ORIGINATING ACTIVITY: Enter the name and address of the contractor, subcontractor, grantee, Department of Defense activity or other organization *(corporate author)* issuing the report.

2a. REPORT SECURITY CLASSIFICATION: Enter the overall security classification of the report. Indicate whether "Restricted Data" is included. Marking is to be in accordance with appropriate security regulations.

2b. GROUP: Automatic downgrading is specified in DoD Directive 5200.10 and Armed Forces Industrial Manual. Enter the group number. Also, when applicable, show that optional markings have been used for Group 3 and Group 4 as authorized.

3. REPORT TITLE: Enter the complete report title in all capital letters. Titles in all cases should be unclassified. If a meaningful title cannot be selected without classification, show title classification in all capitals in parenthesis immediately following the title.

4. DESCRIPTIVE NOTES: If appropriate, enter the type of report, e.g., interim, progress, summary, annual, or final. Give the inclusive dates when a specific reporting period is covered.

5. AUTHOR(S): Enter the name(s) of author(s) as shown on or in the report. Enter last name, first name, middle initial. If military, show rank and branch of service. The name of the principal author is an absolute minimum requirement.

6. REPORT DATE: Enter the date of the report as day, month, year; or month, year. If more than one date appears on the report, use date of publication.

7a. TOTAL NUMBER OF PAGES: The total page count should follow normal pagination procedures, i.e., enter the number of pages containing information.

7b. NUMBER OF REFERENCES: Enter the total number of references cited in the report.

8a. CONTRACT OR GRANT NUMBER: If appropriate, enter the applicable number of the contract or grant under which the report was written.

8b, 8c, & 8d. PROJECT NUMBER: Enter the appropriate military department identification, such as project number, subproject number, system numbers, task number, etc.

9a. ORIGINATOR'S REPORT NUMBER(S): Enter the official report number by which the document will be identified and controlled by the originating activity. This number must be unique to this report.

9b. OTHER REPORT NUMBER(S): If the report has been assigned any other report numbers *(either by the originator or by the sponsor)*, also enter this number(s).

10. AVAILABILITY/LIMITATION NOTICES: Enter any limitations on further dissemination of the report, other than those imposed by security classification, using standard statements such as:

(1) "Qualified requesters may obtain copies of this report from DDC."

(2) "Foreign announcement and dissemination of this report by DDC is not authorized."

(3) "U. S. Government agencies may obtain copies of this report directly from DDC. Other qualified DDC users shall request through

_____."

(4) "U. S. military agencies may obtain copies of this report directly from DDC. Other qualified users shall request through

_____."

(5) "All distribution of this report is controlled. Qualified DDC users shall request through

_____."

If the report has been furnished to the Office of Technical Services, Department of Commerce, for sale to the public, indicate this fact and enter the price, if known.

11. SUPPLEMENTARY NOTES: Use for additional explanatory notes.

12. SPONSORING MILITARY ACTIVITY: Enter the name of the departmental project office or laboratory sponsoring *(paying for)* the research and development. Include address.

13 ABSTRACT: Enter an abstract giving a brief and factual summary of the document indicative of the report, even though it may also appear elsewhere in the body of the technical report. If additional space is required, a continuation sheet shall be attached.

It is highly desirable that the abstract of classified reports be unclassified. Each paragraph of the abstract shall end with an indication of the military security classification of the information in the paragraph, represented as *(TS)*, *(S)*, *(C)*, or *(U)*.

There is no limitation on the length of the abstract. However, the suggested length is from 150 to 225 words.

14. KEY WORDS: Key words are technically meaningful terms or short phrases that characterize a report and may be used as index entries for cataloging the report. Key words must be selected so that no security classification is required. Identifiers, such as equipment model designation, trade name, military project code name, geographic location, may be used as key words but will be followed by an indication of technical context. The assignment of links, rules, and weights is optional.

GPO 884-551